Using Seismic Attributes in seismotectonic research: an application to the Norcia's Mw=6.5 earthquake (30th October 2016) in Central Italy.

Maurizio Ercoli[1;4], Emanuele Forte[2], Massimiliano Porreca[1;4], Ramon Carbonell[3], Cristina Pauselli[1;4], Giorgio Minelli[1;4], Massimiliano R. Barchi[1;4].

[1] Dip. di Fisica e Geologia – Università degli Studi di Perugia (Perugia, Italy).
[2] Dept. of Mathematics and Geosciences, University of Trieste (Trieste, Italy).
[3] Dept. Structure & Dynamics of the Earth, CSIC-Inst. Earth Sciences Jaume Almera (Barcelona, Spain).
[4] Member of Interuniversity Center for Research on 3D-Seismotectonics (Centro InterRUniversitario per l'Analisi SismoTettonica tridimensionale con applicazioni territoriali – CRUST).

Correspondence to: Maurizio Ercoli (maurizio.ercoli@unipg.it; maurizio.ercoli@gmail.com)

Abstract. In seismotectonic studies, seismic reflection data are a powerful tool to unravel the complex deep architecture of active faults. Such tectonic structures are usually mapped at the surface through traditional geological surveying whilst seismic reflection data may help to trace their continuation from the near-surface down to hypocentral depth. In this study, we propose the application of the seismic attributes technique, commonly used in seismic reflection exploration by oil industry, to seismotectonic research for the first time. The study area is a geologically complex region of Central Italy, struck during the 2016-2017 by a long-lasting seismic sequence, including a Mw 6.5 main-shock. A seismic reflection data-set consisting of three vintage seismic profiles, currently the only ones available at the regional scale across the epicentral zone, represents a singular opportunity to attempt a seismic attribute analysis, by running attributes such as the "Energy" and the "Pseudo Relief". Our results are critical, because provide information on the relatively deep structural setting, mapping a prominent, high amplitude regional reflector interpreted as the top of basement, which is an important rheological boundary. Complex patterns of high-angle discontinuities crossing the reflectors have also been identified by seismic attributes. These steep fabrics are interpreted as the expression of fault zones, belonging to the active normal fault systems responsible for the seismicity of the region. Such peculiar seismic signatures of faulting generally well-match with the principal geological and tectonic structures exposed at surface. In addition, we also provide convincing evidence of an important primary tectonic structure currently debated in literature (the Norcia antithetic fault) as well as buried secondary fault splays. This work demonstrates that seismic attribute analysis, even if used on low-quality vintage 2D data, may contribute to improve the subsurface geological interpretation of areas characterized by poor subsurface data availability but high seismic potential.

1 Introduction

Studying the connections between the earthquakes and the faults to which they are associated is a primary assignment of seismotectonics (Allen et al., 1965; Schwartz and Coppersmith, 1984). Clearly, to fill the gap between the exposed geology (including the active "geological faults") and the seismological data (e.g. focal mechanisms, earthquake locations, etc...) which are indicators of the geometry and kinematics of the seismic source at hypocentral depth ("seismological faults", sensu Barchi & Mirabella, 2008), is not an easy task. The recovery of information on the seismogenic structures at the depth is more challenging, primarily due to the lack of high-resolution geophysical data and/or wells stratigraphy, generating high degree of uncertainty, and bringing to contrasting geological models and interpretation.

Different geophysical methods (e.g. Gravimetry, Magnetics, Electric and Electromagnetic such as Magnetotellurics and Ground Penetrating Radar) may contribute to define the stratigraphy and structural setting of the upper crust at different scales. Furthermore, images provided by seismic reflection method are poorly affected by well-known inversion problems typical of the potential methods (Snieder & Trampert, 1999) and are largely the most powerful tool able to produce high-resolution subsurface images. Such type of data, possibly calibrated by deep wells stratigraphy, may provide important constraints to the definition of subsurface geological architecture: these profiles are useful to unveil the deep geometry of active faults from the surface, where they are mapped in the field, down to hypocentral depths. Unfortunately, ex-novo acquisition (possibly 3D) of onshore deep-reflection data for research purposes, is hampered by high costs, environmental problems and complex logistics (e.g. prohibition of dynamite or vibroseis trucks in Natural Parks or urban areas). Significant exceptions are research projects for deep crustal investigations like BIRPS (Brewer et al., 1983), CoCORP (Cook et al., 1979), ECORS (Roure et al., 1989) and CROP (Barchi et al., 1998; Finetti et al., 2001), IBERSEIS (Simancas et al., 2003), ALCUDIA (Ehsan et al., 2014 and 2015). In seismically active regions, old profiles (legacy data) acquired by the industry have been successfully used to connect the active faults mapped at the surface with the earthquakes seismogenic sources depicted by seismological records (Boncio et al., 2000; Bonini et al., 2014; Carvalho et al., 2008; Beidinger et al., 2011; Maesano et al., 2015; Porreca et al., 2018). Legacy seismic lines have in fact some advantages: 1) they are already available from the oil companies 2) they represent a nice source of information in places where new data is difficult to acquire; 3) they can be used to build up and refine geological models. Moreover, such data are often the only available, and are worth to be used in the most appropriate way for constraining the subsurface geological setting and to provide new data on active tectonic structures (see DISS database, Basili et al., 2008). Vintage profiles can therefore significantly contribute to seismo-tectonic researches, even if characterized by intrinsic limitations: i) their location, orientation and acquisition parameters were not specifically designed with this aim; ii) they were collected with seismic technologies and acquisition/processing strategies of some decades ago, producing data with relatively low signal/noise ratio (S/N) and low resolution, especially in comparison to modern data (Manning et al., 2019). In order to improve the data quality and increase the accuracy of the interpretation, two main strategies, ordinarily used by the O&G industry, can be applied on legacy data: 1) reprocessing from

raw data using modern processing strategies and newly performing algorithms and software; 2) use post-stack analysis techniques such as seismic attributes.

An attribute analysis is the easiest, cheapest and fastest strategy to qualitatively emphasize the geophysical features and data properties of reflection seismic data sets, producing benefits particularly in complex geological areas. A seismic attribute is a quantity derived from seismic data (pre-stack and/or post-stack) commonly used to extract additional information that may be unclear in conventional seismic lines. Examples of applications on dense 3D seismic volumes produced impressive results, including identification of ancient river channels or sets of faults at variable scales (Chopra & Marfurt, 2005; Chopra & Marfurt, 2007; Chopra & Marfurt, 2008; Marfurt et al., 2011; Hale, 2013; Barnes, 2016, Iacopini et al., 2016; Marfurt, 2018; Wrona et al., 2018; Di & AlRegib, 2019; Naeini & Prindle, 2019). Different limitations and advantages exist between 2D vs 3D seismic data, extensively discussed by Torvela et al. (2013) and Hutchinson (2016). For these reasons 2D post-stack seismic attribute may not provide the same quality of information than on 3D, being subjected also to possible pitfalls (Marfurt & Alves, 2015; Ha et al., 2019). However, the main point is that in the past, it was common to sample study areas inland by 2D grids of seismic profiles, being the full 3D seismic surveys rare. Hence, it is relevant to extract as much information as possible from such data.

In this work, the selected study area is located between the southeastern part of the Umbria-Marche Apennines and the Laga Domain, in the outer Northern Apennines (central Italy) (e.g. Barchi et al., 2001). This area presents ideal characteristics to test the application of seismic attributes as a new approach in seismotectonics. In the past, several seismic profiles were acquired in this region for hydrocarbon exploration, and were later used to constrain subsurface geological interpretation (Bally et al., 1986; Barchi et al, 1991; Barchi et al., 1998; Ciaccio et al., 2005; Pauselli et al., 2006; Mirabella et al. 2008; Barchi et al., 2009; Bigi et al., 2011). After the 2016-2017 seismic sequence, Porreca et al. (2018) provided an updated regional geological model based on the interpretation of vintage seismic lines, but remarked important differences in the seismic data quality across the region, hampering a straightforward seismic interpretation. Therefore, the present work exploits the use of seismic attributes on three low-quality seismic profiles located close to the Mw 6.5 main-shock of the 2016-2017 seismic sequence. The main goal is to squeeze additional information from the 2D data obtaining as much constraints as possible on the geological structures responsible for the seismicity in the area by defining:

- geological/structural setting at depth (e.g. depth of the basement and its involvement)

- trace of potentially seismogenic faults (connection between the active faults mapped at the surface and earthquake's foci).

Any improvements achievable on the data quality and visualization, for example an increase of the resolution and/or an enhancement of the lateral discontinuity of seismic reflectors, would represent a valuable contribution considering the limited data availability in this area. We think that this innovative approach to seismotectonic research can be extended to other on-shore seismically active areas in the world, especially if covered only by sparse vintage low-quality seismic surveys. In such cases, we think the seismotectonic research may benefit of the potential and improvements generated by the seismic attributes.

2 Geological framework and seismotectonics of the study area

The study area is located in the southeastern part of the Northern Apennines fold and thrust belt, including the Umbria-Marche Domain and the Laga Domain, separated by an important regional tectonic structure, known as the M. Sibillini thrust (MSt) (Fig. 1). The Umbria-Marche domain involves the rocks of the sedimentary cover, represented by three main units (top to bottom), characterized by different interval velocities (Bally et al., 1986; Barchi et al., 1998; Porreca et al., 2018): 1) on top, the Laga sequence (Late Messinian – Lower Pliocene, up to 3000 m thick, average seismic velocity; V_{av} = 4000 m/s), consisting of siliciclastic turbidites made by alternating layers of sandstones, marls and evaporites, deposited in marine depositional environment (Milli et al., 2007; Bigi et al., 2011); it is and outcropping in the eastern sector of the study area (i.e. Laga Domain); 2) the carbonate formations (Jurassic-Oligocene, about 2000 m thick, V_{av} = 5800 m/s), formed by pelagic limestones (Mirabella et al., 2008) with subordinated marly levels overlying an early Jurassic carbonate platform (Calcare Massiccio Fm.), mainly outcropping in the Umbria-Marche Domain; 3) the Late Triassic evaporites (1500–2500 m thick, V_{av}= 6400 m/s), consisting in alternated layers of anhydrites and dolomites (Anidriti di Burano Fm. and and Raethavicula Contorta beds; Martinis & Pieri, 1964), never outcropping and intercepted only by deep wells (Porreca et al., 2018 and references therein). For further details on the stratigraphic characteristics of the area, we remind to the works of Centamore et al. (1992) and Pierantoni et al. (2013).

These units rest on a basement with variable lithology (Permian-Late Triassic, V_{av} = 5100 m/s) that never crops out in the study area (Vai, 2001), but only intercepted by deep wells (Bally et al., 1986; Minelli & Menichetti, 1990; Anelli et al., 1994; Patacca & Scandone, 2001).

This sedimentary sequence is involved in the Late Miocene fold and thrust belt including a set of N-S trending anticlines, formed at the hangingwall of the W-dipping arc-shaped major thrusts. The most important compressional structure is the M. Sibillini thrust (MSt, Koopman, 1983; Lavecchia, 1985), where the Umbria-Marche Domain is overthrusted on the Laga Domain.

This is a geologically complex region, where in the past the analysis of 2D seismic profiles have produced contrasting interpretations of the upper crust structural setting, i.e. thin- vs. thick-skinned tectonics, fault reactivation/inversion and basement depth (Bally et al., 1986; Barchi, 1991; Barchi et al., 2001; Bigi et al., 2011; Calamita et al., 2012). A review of the geological history of this area has recently been provided by Porreca et al. (2018). These authors propose a tectonic style characterized by coexistence of thick- and thin-skinned tectonics with multiple detachments localized at different structural levels.

These compressional structures have been later disrupted by the extensional faults since the Late Pliocene (Fig.1) (Blumetti et al., 1993; Boncio et al., 1998; Brozzetti & Lavecchia, 1994; Calamita & Pizzi, 1994; Pierantoni et al., 2013). The Late Pliocene-Quaternary extensional tectonic phase, characterized by NNW-SSE striking normal faults, consistent with the present-day active strain field as deduced by geodetic data (e.g. Anderlini et al., 2016). The latter have high dip angles (50-70°) and can be synthetic or antithetic structures (WSW or ENE dipping, respectively) dipping normal faults. These

129 faults were also responsible of the tectono-sedimentary evolution of intra-mountain continental basins (Calamita et al., 1994;

130 Cavinato and De Celles, 1999). The most evident Quaternary basins of this part of the Apennines are the Castelluccio di

131 Norcia and Norcia basins (Fig.1), located at 1270 and 700 m a.s.l., here named CNb and Nb respectively. A phase of

132 lacustrine and fluvial sedimentation infilled the two basins with hundred meters of deposits, characterized by fine clayey to

133 coarse grained material (Blumetti et al., 1993; Coltorti and Farabollini, 1995).

134 The area is affected by frequent moderate magnitude earthquakes (5 < Mw < 7) and has a high seismogenic potential

135 revealed by both historical and instrumental data (e.g. Barchi et al., 2000; Boncio and Lavecchia, 2000; Basili et al., 2008;

136 Rovida et al., 2016; DISS Working Group, 2018).

137 The major seismogenic structures recognized in the area are the Norcia fault (Nf) and the M. Vettore fault (Vf). The Norcia

138 fault (Nf, Fig.1) is associated to several historical events (Galli et al., 2015; Pauselli et al., 2010; Rovida et al., 2016),

139 probably including the 1979 earthquake (Nottoria-Preci fault, Deschamps et al., 1984; Brozzetti & Lavecchia, 1994; Rovida

140 et al., 2016) and the largest event in 1703 (Me = 6.8, Rovida et al., 2016). The Vettore fault (Vf) in part of the easternmost

141 alignment whose historical and pre-historical activity was recognized by paleoseismological and shallow geophysical

142 surveys (Galadini & Galli, 2003; Galli et al., 2008; Ercoli et al., 2013; Ercoli et al., 2014; Galadini et al., 2018; Galli et al.,

143 2018; Cinti et al, 2019; Galli et al., 2019). This system was reactivated during the 2016-2017 sequence characterized by

144 multi-fault ruptures occurred within few months (nine M>5 earthquakes at hypocentral depth < 12 km between August 2016

145 – January 2017) having characteristics comparable to previous seismic sequences in Central Italy (e.g. L'Aquila 2009 and

146 Colfiorito 1997-1998, Valoroso et al., 2013 and Chiaraluce et al., 2005).

147 The strongest mainshock of (Mw 6.5) occurred on 30th October 2016 (Chiaraluce et al., 2017; Chiarabba et al., 2018;

148 Gruppo di Lavoro Sequenza Centro Italia, 2019; Improta et al., 2019; ISIDe working group, 2019), generating up to 2 m

149 (vertical offset) co-seismic ruptures (Civico et al., 2018; Gori et al., 2018; Villani et al., 2018a; Brozzetti et al., 2019),

150 mainly localized along the Mt. Vettore fault (blue thin lines in Fig. 1).

151 Despite of the large amount of surface data collected (Livio et al., 2016; Pucci at al., 2017; Wilkinson et al., 2017; De Guidi

152 et al., 2017; Brozzetti et al., 2019), the deep extension of the Norcia and Castelluccio antithetic and synthetic faults

153 (particularly Nf and Vf), and the overall complex structure of the area are still debated (Lavecchia et al., 2016; Porreca et al.,

154 2018; Bonini et al., 2019, Cheloni et al., 2018, Improta et al. 2019).

155 **3 Data**

156 We have performed seismic attributes analysis on three W-E trending 2D seismic reflection data crossing the epicentral area

157 between the Umbria and Marche regions (Central Italy, Fig.1). These seismic profiles are part of a much larger, unpublished

158 dataset including 97 seismic profiles and few boreholes, drilled for hydrocarbon exploration by ENI in the period 1970-1998.

159 The data quality is extremely variable (medium/poor) with limited fold (generally < 60 traces / Common Mid-Point), mainly

160 due to environmental and logistical factors. Among those, we can list the different acquisition technologies, a limited site

161 access, the complex tectonic setting and especially the different (contrasting) outcropping lithologies (e.g. Mazzotti et al.,

162   2000, Mirabella et al., 2008). The eastern area, showing higher data quality, consists of siliciclastic units of the Laga

163   foredeep sequence, located at the footwall of the MSt. On the contrary, the lowest S/N recordings coincide with outcropping

164   carbonates formations and Quaternary deposits.

165   The analysed lines include seismic reflection profiles NOR01 (stack, 14 km long) and NOR02 (time-migrated, 20 km long,

166   partially parallel to NOR01 on the western sector) located west and east to the Nb, respectively; CAS01 (stack, 16 km long),

167   located more to the south crossing the Cascia village (Fig. 1).

168   NOR01 and CAS01 were acquired using a Vibroseis source, whilst explosives were used for NOR02; all the lines are

169   displayed in Two-Way-Travel-Time (TWTT) limited to 4.5 s. The amplitude/frequency spectra (computed on the entire time

170   window) of the processed lines show a bandwidth in a range 10-50 MHz, with the NOR02 spectrum displaying a slighter

171   high frequency content (Tab.1). Assuming the average peak frequency of 20 Hz, a vertical resolution of ca. 80 m can be

172   estimated (average carbonate velocity = 6 km/s; parameters in Table 1). Some processing artefacts are visible in NOR01 as a

173   straight horizontal signal at ca. 1 s (yellow dashed line and label A in Fig. 2a), and another in CAS01 (Fig. 3a). The data

174   display may benefit of potential improvements by selecting seismic attributes to be tested with different calculation

175   parameters. Therefore, we loaded the lines into the software OpendTect (OdT,

176   https://www.dgbes.com/index.php/software#free), setting up a common seismic datum of 500 m. Unfortunately, deep

177   borehole stratigraphy is not available for the study area (all details about surrounding deep wells have been already

178   summarized in Porreca et al., 2018). The OdT seismic project was enriched also by ancillary data, extracted by a

179   complementary GIS project (QGis, https://www.qgis.org/it/site/). As visible in Fig. 1, we have included a detailed summary

180   of the main normal faults and surface ruptures of the area (Civico et al., 2018; Villani et al., 2018a; Brozzetti et al., 2019),

181   obtained after carefully checking the most important regional geological maps and fault patterns (Koopman, 1983;

182   Centamore et al., 1993; Pierantoni et al., 2013; Carta Geologica Regionale 1:10'000 – Regione Marche, 2014; Carta

183   Geologica Regionale 1:10'000 – Regione Umbria, 2016; Ithaca database, http://www.isprambiente.gov.it/it/progetti/suolo-e-

184   territorio-1/ithaca-catalogo-delle-faglie-capaci;), as well as the most recent works published in literature (e.g. Brozzetti et al.,

185   2019; Porreca et al., 2020). The topography was also included using a regional 10 meters resolution DTM (Tarquini et al.,

186   2007; Tarquini et al., 2012). The other important external data-set consists of seismological data, i.e. inferred location and

187   approximated fault geometry as suggested by the focal mechanisms of the mainshocks and by the distribution of the

188   aftershocks (Iside database, http://iside.rm.ingv.it/iside/ and Chiaraluce et al., 2017). The integration of such information in a

189   pseudo-3D environment offered us a multidisciplinary platform to clearly display the seismic lines and to link surface data

190   and the deep geologic structures at hypocentral depth.

191   **4 Methods**

192   The seismic reflection data interpretation is generally accomplished through the definition of specific signal characteristics

193   (seismic signature), supported by the geological knowledge of the study area. A standard seismic interpretation is affected by

194   a certain degree of uncertainty/subjectivity (particularly in case of poor data quality), because is generally based on a

qualitative analysis of amplitude, geometry and lateral continuity of reflections. Over the last years, the introduction of seismic attributes and related automated/semi-automated procedures had an important role in reducing the subjectivity of seismic interpretation. A seismic attribute is a descriptive and quantifiable parameter that can be calculated on a single trace, on multiple traces, or 3D volumes and can be displayed at the same scale as the original data. Seismic data can be therefore considered a composition of constituent attributes (Barnes, 1999, Taner et al., 1979, Forte et al., 2012). Their benefits have been first appreciated in 2D/3D seismic reflection data (Barnes 1996; Taner et al., 1979; Barnes, 1999; Chen and Sidney, 1997; Taner, 2001; Chopra and Marfurt, 2007; Chopra and Marfurt, 2008; Iacopini and Butler, 2011; Iacopini et al., 2012; McArdle et al., 2014; Botter et al., 2014; Hale, 2013 for a review; Marfurt and Alves, 2015; Forte et al., 2016) and, more recently, also in other reflection techniques like the Ground Penetrating Radar (e.g. McClymont et al., 2008; Forte et al., 2012; Ercoli et al., 2015, Lima et al., 2018). In this work, we have tested several post-stack attributes on three 2D vintage seismic lines (original seismic data in the supplementary material in Fig.1s), and starting our analysis by using first well-known and widely used attributes like the instantaneous amplitude, phase, frequency, and their combinations, also using composite multi-attribute (i.e. simultaneous overlay and display of different attributes e.g. primarily phase, frequency, envelope; Chopra and Marfurt, 2005; Chopra and Marfurt, 2011). Later on, we have also tested attributes (e.g. coherency and similarity, generally more efficient on 3D volumes) but without obtaining positive outcomes, due to limited vertical and spatial resolution of the data. Among tested attributes, we selected three attributes that resulted in the best images (provided in Figs. s2, s3 and s4 of the supplementary material without any line drawing or labels), making possible to detect peculiar seismic signatures of regional seismogenic layers and fault zones. The attributes, computed using OdT software, are:

"Energy" (EN): one of the RMS amplitude-based attributes, it is defined as the ratio between the squared sum of the sample values in a specified time-gate and the number of samples in the gate (Taner, 1979, Gersztenkorn & Marfurt, 1999, Chopra & Marfurt, 2005, Chopra & Marfurt, 2007, for a review of formulas see Appendix A in Forte et al., 2012). The Energy measures the reflectivity in a specified time-gate, so the higher the Energy, the higher is the reflection amplitude. In comparison to the original seismic amplitude, it is independent of the polarity of the seismic data being always positive, and in turn preventing the zero-crossing problems of the seismic amplitude (Forte et al., 2012, Ercoli et al., 2015, Lima et al., 2018, Zhao et al., 2018). This attribute is useful to emphasize the most reflective zones (e.g. characterization of acoustic properties of rocks). It may also enhance sharp lateral variations in seismic reflectors, highlighting discontinuities like fractures and faults. In this work, we set a 20 ms time window (i.e. about the mean wavelet length), obtaining considerable improvements in the visualization of higher acoustic impedance contrasts.

"Energy gradient" (EG): it is the first derivative of the energy with respect to time (or depth). The algorithm calculates the derivative in moving windows and returns the variation of the calculated energy as a function of time or depth (Chopra & Marfurt, 2007; Forte et al., 2012). It is a simple and robust attribute, also useful for a detailed semi-automatic mapping of horizons with a relative low level of subjectivity. The attribute acts as an edge detection

229 tool, effective in the mapping of the reflection patterns as well as the continuity of both steep discontinuities like

230 faults and fractures, and channels, particularly in slices of 3D data (Chopra & Marfurt, 2007). In this work, we have

231 used the same time window of the Energy, obtaining considerable improvements in the visualization not only of the

232 strong acoustic impedance reflectors but particularly in the faults imaged in the shallowest part of the seismic

233 sections.

234 **Pseudo-relief (PR):** it is obtained in two steps: the energy attribute is first computed in a short time window, then

235 followed by the Hilbert transform (phase rotation of -90 degrees). The Pseudo-relief is considered very useful in 2D

236 seismic interpretation to generate "outcrop-like" images allowing an easier detection of both faults and horizons

237 (Bulhões, 1999; Barnes et al., 2011; Vernengo et al. 2017, Lima et al., 2018). In this work, considerable display

238 improvements have been obtained using the Pseudo-relief computed in a window of 20 ms. In comparison to the

239 standard amplitude, it better highlights the reflection patterns and thus the continuity/discontinuity of reflectors,

240 enhancing steep discontinuities and fault zones.

5 Results

242 The Figs. 2, 3 and 4 show the comparison between the original seismic lines in amplitude and the images obtained after the

243 attribute analysis, revealing significant improvements in the visualization and interpretability of the geophysical features. In

244 the profiles NOR01, CAS01 and NOR02 we focus our analysis on three types of geophysical features highlighted by the

245 attributes: sub-horizontal deep reflectors, low-angle and high-angle discontinuities. The main faults known at the surface

246 (Fig.1) have been also plotted on top of each seismic line.

247 In the original seismic line NOR01 (Fig. 2a), the overall low S/N ratio hampers the detection of clear and continuous

248 reflectors. At ca. 1 s a horizontal processing artefact is visible (label A, yellow dots), possibly related to a windowed filter.

249 The most prominent sub-horizontal reflections (labelled H) are located in the central portion between 2-3 s (TWT) (strong

250 reflectors in the black box i). Shallower and less continuous reflectors are also visible in the eastern side of the profile,

251 beneath the Nb (black box ii). The EN attribute (Fig. 2b) enhances the reflectivity contrast, better focusing the high-

252 amplitude, gently W-dipping reflector H (blue arrows) and also outlining its lateral extension. In this image most of the

253 reflected energy is concentrated on its top at ca. 2.5 s, so that it is readily apparent that H separates two seismic facies, with

254 higher (top) and lower (bottom) amplitude response, respectively. The EG and PR attributes of NOR01 (Figs. 2c, 2d) better

255 show the geometry of horizon H, characterized by a continuous, ca. 8 km long, package of reflectors (ca. 200 ms thick)

256 having common characteristics in terms of reflection strength and period. In the eastern part of the profile, below the Nb, the

257 EG and PR attributes also enhance two major opposite-dipping high-angle geophysical features (red arrows in fig. 2c and

258 2d), crossing and disrupting the shallower reflectors. The W-dipping lineament propagates down to ca. 2.5 s, intercepting the

259 eastern termination of the reflector H. The two discontinuities border a relatively transparent, shallow seismic facies,

260 corresponding to the area where the Nb crops out. In the same area, the reflectors are pervasively disrupted by other, minor

261 discontinuities.

The original seismic reflection line CAS01 (Fig. 3a) displays a generalized high-frequency noise content. As in NOR01, a shallow processing artefact (A, yellow dots) is visible and possibly related to a filter. Fragmented packages of high-amplitude reflectors (H) are visible at the same time interval observed in NOR01 (ca. 2.5 s), in both the western (black box i, in Fig. 3a) and, more discontinuous, in eastern part of the line (black box ii, in Fig. 3a). The EN attribute (Fig. 3b) emphasizes the presence of the H reflector better focusing the reflectivity (blue arrows). Both the EG and PR attributes (Figs. 3c and 3d) further help to delineate the reflector H. The steeper discontinuities have been analysed mainly in the western part of the profile, closer to the 2016-2017 seismically active area. A major high-angle, east-dipping discontinuity has been traced at about 13 km (alignment of red arrows in Fig. 3c and 3d).

The original seismic line NOR02 (Fig. 4a), displays geophysical features similar to the ones detected in NOR01 and CAS01. This seismic profile shows a generalized poor continuity of the reflectors, with the exception of the eastern side, where a set of west-dipping, coherent reflections can be recognized: the higher S/N ratio of this part of the section is due to the outcropping turbidites of Laga sequence, which are known to favour the energy penetration, respect to the carbonates (e.g. Bally et al., 1986; Barchi et al., 1998). The prominent reflection H, gently east-dipping and relatively continuous for more than 8 km (black box in Fig 4a), is located in the centre of the line, at greater depth (3.2–3.5 s TWT), respect to the previously described NOR01 and CAS01 profiles. As in the previous cases, the EN attribute (Fig. 4b) effectively focuses the horizons reflectivity, emphasising the strong amplitude of the reflector H (blue arrows). The EG and PR attributes (Figs. 4c and 4d) improve the overall visualization of the reflection patterns, aiding the detection of the low-angle and high-angle discontinuities. A major westward low-angle discontinuity T (green dots in Figs.4c and 4d) crosses the entire profile, descending from ca. 2 s (East) to ca. 4 s (West), where it interrupts marks the continuity of the reflector H. Several high-angle discontinuities have been traced along the section, marked by alignments of red arrows in Figs. 4c and 4d. The most important alignments have been recognised beneath the two major Quaternary basins (i.e. Nb and CNb) crossed by the profile: in both cases, major W-dipping alignments can be traced from the near surface, where they correspond to the eastern border of the above mentioned basins, down to a depth of ca. 4 s TWT. Other discontinuities, W and E dipping, have been traced in the hanging-wall of these two major alignments. In the seismic volume bounded by these features, many secondary (minor) discontinuities pervasively cross-cut the set of reflectors, producing a densely fragmented pattern. Unfortunately, limited resolution and data quality in the deeper part of the section hampers a univocal interpretation of the cross-cutting relationships between the low-angle discontinuity T and the major W-dipping high-angle discontinuity: two alternative interpretations are here possible, that will be discussed in detail in the next paragraph 6.

The global improvement in the dataset interpretability can be better appreciated in a 3D visualization of the seismic attributes, also using multi-attribute displays (Fig. 5). Such images better clarify the deep geometry of the main reflectors and the location of the geophysical discontinuities, later interpreted on the light of known and debated tectonic structures on the study area. In Fig. 5a we report a 3D perspective of the seismic line NOR02, after combining in transparency the EN attribute with the PR attribute (EN+PR). The reflectors characteristics and a pattern of discontinuities are clearly visible at different levels of detail, and the link with the faults at surface is again proposed (red segments on the top). The two boxes

296 (blue and black colours in Fig.5a, respectively) point out the two most representative seismic facies described above. The

297 Fig. 5b and 5c display a comparison of the signature of reflector H in the standard amplitude line (SA) (Fig. 5b) and in a

298 version including PR attribute in transparency with SA itself. Again, in the inserts Figs. 5d and 5e, an analogous data

299 comparison shows the scarce detectability of the dense pattern of steep discontinuities in the original seismic profile. The

300 Fig.5e displays the enhancement obtained plotting the PR attribute plus SA in transparency, greatly improving the

301 visualization of the dense reflectors' fragmentation.

302 An analogous 3D multi-display of attributes EN and PR is proposed in Fig. 6a for the seismic line NOR01. The comparison

303 between the original line (blue box in Fig. 6b) and the EN+PR (Fig. 6c) shows the improved and peculiar signature of the

304 strong reflector H. The black box again reports the original plot *vs.* the PR+SA, which clearly boost the visualization of the

305 high-angle discontinuities.

306 6 Data Interpretation: new elements and insights on the deep geological structure of the study area.

307 The comparison between the original seismic data and the images obtained by the attribute analysis ensures an easier and

308 accurate interpretation of the geophysical features, allowing to extend the surface geological data in depth. The geological

309 interpretation of these features requires a thoughtful comparison and calibration with the other data available for the area,

310 e.g. geological and structural maps, co-seismic ruptures, high-resolution topography and mainshocks hypocentres. The

311 seismic attributes provide a multiple view of the original data through the enhancement of different physical quantities.

312 Therefore, peculiar geophysical signatures have been detected delineating interpretative criteria (e.g. high amplitude

313 reflectors, phase discontinuities, fragmented reflectors patterns etc…). Such geophysical features, after a first order

314 interpretation, fit well with the main outcropping geologic structures. Using the same interpretation criteria, other surface-

315 uncorrelated discontinuities, poorly visible in the original amplitude lines, are apparent at a more detailed scale after the

316 attributes analysis. In addition, deep reflectors showing a common signature have been also recognized, revealing a regional

317 character. The geological meaning and the relation of such geophysical features with the surface geology and with the

318 hypocentre location of the main earthquakes are hereafter discussed.

319 Fig. 7 reports a global pseudo-3D view of the study region summarizing all the data analysed across the area, together with

320 all the faults mapped at surface (Fig. 7a) and the location of Mw 6.5 mainshock (30th October 2016). The two seismic

321 images in Figs. 7b and 7c have been obtained using again a multi-attributes visualization, overlapping the PR and EN

322 attributes in transparency with the original seismic lines NOR01 and NOR02, following the same procedure used for the

323 images in Figs. 5 and 6. The Figs. 7d and 7e propose an interpretation of the geophysical features being associated to the

324 faults highlighted after an accurate analysis of the discontinuities of attributes signatures, as shown in fig. s5. Regarding the

325 deeper parts of the sections, the reflector H (blue arrows and dashed line) highlighted in NOR01 (and in CAS01), presents a

326 seismic character and an attribute signature compatible with the deeper reflector of NOR02 beneath CNb. This set of

327 reflectors is interpreted as a high acoustic impedance contrast, possibly related to an important velocity inversion occurring

328 between the Triassic Evaporites (anhydrites and dolostones, $Vp \approx 6$ km/s, e.g. Trippetta et al., 2010) and the underlying

329 acoustic Basement (metasedimentary rocks, Vp ≈ 5 km/s, sensu Bally et al., 1986). Comparable deep and prominent

330 reflectors were detected also in other legacy data across adjacent regions of the Umbria-Marche Apennines (e.g. Barchi et

331 al., 1998; Mirabella et al., 2008). This fact confirms its regional importance, particularly because it represents a lithological

332 control marking a seismicity cutoff (Chiaraluce et al., 2017; Mirabella et al., 2008; Porreca et al., 2018; Mancinelli et al.,

333 2019).

334 As already pointed out in the previous figures, the continuity of the deep reflector H is interrupted in the western edge by the

335 low-angle west-dipping discontinuity T crossing NOR02 (Fig. 7e), and not identified in the interpretation by Porreca et al.

336 (2018). This deep discontinuity can be interpreted as a regional thrust emerging at the footwall of the MSt, in an easternmost

337 sector of the region, and corresponding to the Acquasanta thrust (Centamore et al., 1993).

338 In NOR01, the most visible high-angle seismic discontinuity is marked by an E-dipping fault, bordering the western area of

339 Nb (Fig. 7d). The location and geometry of this fault, whose presence is still debated in literature, perfectly match its

340 supposed position at surface (Blumetti et al., 1993; Pizzi et al., 2002; Galadini et al., 2018; Galli et al., 2018). Therefore, it

341 may represent the first clear geophysical evidence at depth of the antithetic normal fault of Norcia (aNf), suggested by

342 morphological studies (Blumetti et al., 1990) and paleoseismological records (Borre et al., 2003) and belonging to a

343 conjugate tectonic system (Brozzetti & Lavecchia, 1994; Lavecchia et al., 1994).

344 The other principal structure is a synthetic (W-dipping) high-angle, normal fault bordering the eastern flank of Nb

345 ("Nottoria-Preci fault" – Nf, Calamita et al., 1982; Blumetti et al., 1993; Calamita & Pizzi, 1994). The Nf in NOR02 is

346 marked by a downward propagation of a steep alignment (continuous red line in Fig. 7d). This area is also fragmented by

347 several minor strands parallel to the main faults (dashed lines in Fig. 7d). In particular, several west-dipping minor faults are

348 observed in Fig. s5a, where the shallower high-amplitude reflectors of the PR attribute are clearly disrupted.

349 Another discontinuity interpretable as a deep fault is visible slightly eastward, close to the mainshock hypocentral location

350 (Fig. 7e). This E-dipping discontinuity, emphasized by the attribute analysis, does not reach the surface. The presence of this

351 blind fault has been suggested by several authors in relation to the occurrence of an aftershock (Mw 5.4), which "ruptured a

352 buried antithetic normal fault on eastern side of Nb, parallel to the western bounding fault of CNb" (Chiaraluce et al., 2017,

353 Porreca et al., 2018 and Improta et al., 2019).

354 The central portion of NOR02, corresponding to CNb, shows a peculiar reflection fabric, dominated by high-angle

355 discontinuities, interpreted as two opposite-dipping normal faults bordering the basin, well matching their positions mapped

356 at surface (cfr. Pierantoni et al., 2013). The main fault is here represented by the W-dipping Vf, reactivated during the 2016

357 earthquake (e.g. Villani et al., 2018a) which can be traced from its surface expression downward to hypocentre location.

358 Parallel to the Vf, several high-angle seismic discontinuities representing minor normal faults cross-cut the gently W-dipping

359 reflectors (Fig. 7e, further details in Fig. s5).

360 Analogous considerations can be extended to a multitude of E-dipping steep discontinuities at the westward side of CNb.

361 These may represent the evidence of an antithetic fault (aVf), and several minor fault strands characterized by high-angle dip

362 at shallow depths (Villani et al., 2018b). Such a fault appears connected at about 2-3 s to the W-dipping master Vf,

363 producing a conjugate system geometry like observed at Nb (Fig. 8e). At depth of 3.2 s, Vf fault clearly interrupt the

364 continuity of the top basement reflector H, whilst the relationships with the Acquasanta thrust (low-angle discontinuity T) is

365 more ambiguous. Two alternative interpretations can be proposed, schematically represented in Fig. 8. In Fig. 8a, we

366 propose a model in which Vf merges into the deep Acquasanta thrust, suggesting a negative inversion, as a mechanism

367 proposed by other authors (e.g. Calamita and Pizzi, 1994; Pizzi et al., 2017; Scognamiglio et al., 2018). In Fig. 8b, Vf cuts

368 and displaces the Acquasanta thrust, following a steeper trajectory (ramp) (Lavecchia et al., 1994 and Porreca et al., 2018).

369 For both Norcia and Castelluccio di Norcia basins, the interpreted data suggest two slightly asymmetric fault systems, due to

370 conjugate sets of seismogenic master faults (Ramsay & Huber, 1987) producing a "basin-and-range" morphology (Serva at

371 al., 2002), progressively lowering the topography from east to west, and forming two major topographic steps, corresponding

372 to the CNb and Nb, respectively. Such fault systems control the evolution of the continental basins, and are associated with

373 several complex sets of secondary strands building up complex fault zones. Such fault strands are able to produce surface

374 ruptures in future earthquakes, as occurred in the 2016-2017 seismic swarm, and would require further studies through high-

375 resolution geophysical investigations (e.g. Bohm et al., 2011 and Villani et al. 2019).

376 The results of the seismic interpretation proposed in this work, supported by the attribute analysis, suggests that such

377 synthetic and antithetic tectonic structures at the Norcia and Castelluccio di Norcia basins cannot be actually simplified as a

378 unique fault plane, but they could be imaged as complex and fractured fault zones, like also conceived also by Ferrario &

379 Livio (2018) as "distributed faulting and rupture zones".

Conclusions

381 Taking into account the important role that seismic attributes play in the O&G industry, their usage might be of high interest

382 also for improving the geological interpretation of vintage seismic data, aimed to scientific purposes. When applied to

383 seismically active areas, this analysis may contribute to constrain the buried geological setting and, combined with

384 seismological data (i.e. focal mechanisms and accurate earthquake locations), may have high potential impact for the

385 identification and characterization of the seismogenic sources and eventually on earthquakes hazard assessment.

386 This contribution presents one of the first case studies where the seismic attribute analysis is used for seismotectonic

387 purposes. The analysis is applied to seismic reflection data collected more than 30 years ago in Central Italy. Such industrial

388 data, nowadays irreproducible in regions where the seismic exploration is forbidden, represent, despite the limited quality, a

389 unique source of information on the geological setting at depth.

390 This contribution reveals that the use of seismic attributes can improve the interpretation for the subsurface assessment and

391 structural characterization. Certainly, the overall low quality of the data sets did neither allow to extract rock petrophysical

392 parameters, nor more quantitative information. However, the attributes aid the seismic interpretation to better display the

393 reflection patterns of interest and provided new and original details on complex tectonic region in Central Italy. Our attribute

394 analysis considerably improved the overall interpretability of the vintage seismic lines crossing the epicentral area of the

395 2016-2017 Norcia-Amatrice seismic sequence. In particular, we detected peculiar seismic signatures of a deep horizon of

396 regional importance, corresponding, most probably, to the base of the seismogenic layer, and to the location and geometry of

397 the complex active fault zones. Those consists of several secondary synthetic and antithetic splays in both the Quaternary

398 basins, generally consistent with its surface location, but also reinforcing the existence of several faults with no clear surface

399 outcrop, issue currently much debated in the literature.

400 The analysis and integration of the seismic attributes allowed the determination of the deep continuation of the (known and

401 supposed) faults and, the recently mapped co-seismic ruptures at surface, providing a pseudo-3D picture of the buried

402 structural setting of the area. The seismic attributes may help to reduce the gap between the surface geology and deep

403 seismological data, also revealing a high structural complexity at different scales, which cannot generally be detected only

404 by using traditional interpretation techniques. This approach has shown the potential of the attribute analysis, that even when

405 applied on 2D vintage seismic lines, may significantly extend the data value. For all these reasons, we strongly encourage its

406 application for seismotectonic research, aimed to provide new information and additional constraints across other seismically

407 active regions around the world.

Acknowledgments

409 We are grateful to Eni S.p.A. for providing an inedited set of seismic reflection lines after the 2016-2017 seismic crisis in
410 Central Italy (raw data available in Fig.2 of supporting information). The original seismic reflection lines used in this study
411 are available in the supplementary material, well as the high-resolution Figures 2,3,4,7. The authors are very grateful to dgB
412 Earth Sciences and to QGIS teams for providing the academic software used in this work. We thank Dr. Christian Berndt and
413 Dr. David Iacopini for their valuable comments provided for this paper. We also thank the two anonymous reviewers for
414 their patience in providing useful suggestions and detailed corrections that considerably improved this work.

References

Allen, C. R., St. Amand, P., Richter, C. F., & Nordquist, J.: Relationship between seismicity and geologic structure in the southern California region. Bulletin of the Seismological Society of America, 55(4), 753-797, 1965.

Anderlini, L., Serpelloni, E., and Belardinelli, M. E.: Creep and locking of a low-angle normal fault: Insights from the Altotiberina fault in the Northern Apennines (Italy), Geophys. Res. Lett., 43, 4321– 4329, doi:10.1002/2016GL068604, 2016.

Anelli, L., Gorza, M., Pieri, M., and Riva, M.: Subsurface well data in the Northern Apennines (Italy). Memorie della Società Geologica Italiana, 48, 461–471, 1994.

Bally, A. W., Burbi, L., Cooper, C., & Ghelardoni, R.: Balanced cross-sections and seismic reflection profiles across the central Apennines. Memorie della Societa Geologica Italiana, 35, 257–310, 1986.

Barchi, M.: Integration of a seismic profile with surface and subsurface geology in a cross-section through the Umbria-Marche Apennines. Bollettino della Società Geologica Italiana, 110, 469–479, 1991.

Barchi, M. R., Minelli, G. and Pialli, G.: The CROP 03 Profile: a synthesis of results on deep structures of the Northern Apennines, Mem. Soc. Geol. It., 52, 383-400, 1998.

Barchi M.R., Galadini, F., Lavecchia, G., Messina, P., Michetti, A. M., Peruzza, L., Pizzi, A., Tondi & Vittori, E.: Sintesi delle conoscenze sulle faglie attive in Italia Centrale: parametrizzazione ai fini della caratterizzazione della pericolosità sismica. CNR-Gruppo Nazionale per la Difesa dai Terremoti, Roma, 62 pp., 2000.

Barchi, M., Landuzzi, A., Minelli, G., & Pialli, G.: Outer northern Apennines. In anatomy of an orogen: The Apennines and adjacent Mediterranean Basins. Netherlands, Springer, 215–253, 2001.

Barchi, M. R., & Mirabella, F.: The 1997-98 Umbria-Marche earthquake sequence: "Geological" vs. "seismological" faults. Tectonophysics, 476(1–2), 170–179. https://doi.org/10.1016/j.tecto.2008.09.013, 2008.

Barnes, A. E.: Theory of two-dimensional complex seismic trace analysis. Geophysics, 61, 264–272, 1996.

Barnes, A. E.: Attributes for automating seismic facies analysis. Seg Technical Program Expanded Abstracts, 19. doi:10.1190/1.1816121, 1999.

Barnes, A. E.: "Displaying Seismic Data to Look Like Geology", chapter of: "Attributes: New Views on Seismic Imaging– Their Use in Exploration and Production", Marfurt, K. J. Gao, D., Barnes, A., Chopra, S., Corrao, A., Hart, B., James, H., Pacht, J., Rosen, N.C. (2011), SEPM Society for Sedimentary Geology, 31, doi: 10.5724/gcs.11.31, 2011.

Barnes, A., E.: Handbook of Poststack Seismic Attributes, Society of Exploration Geophysicists, 21, doi: 10.1190/1.9781560803324, 2016.

Basili, R., Valensise, G., Vannoli, P., Burrato, P., Fracassi, U., Mariano, S., ... & Boschi, E.: The Database of Individual Seismogenic Sources (DISS), version 3: summarizing 20 years of research on Italy's earthquake geology. Tectonophysics, 453(1-4), 20-43, 2008.

447 Beidinger, A., Decker, K., & Roch, K. H.: The Lassee segment of the Vienna Basin fault system as a potential source of the
448 earthquake of Carnuntum in the fourth century AD. International Journal of Earth Sciences, 100(6), 1315-1329, 2011.

449 Bigi, S., Casero, P., & Ciotoli, G.: Seismic interpretation of the Laga basin; constraints on the structural setting and
450 kinematics of the central Apennines. Journal of the Geological Society, 168(1), 179–190. doi 10.1144/0016-76492010-084,
451 2011.

452 Blumetti, A.M., Coltorti, M., Dramis, F., Farabollini, P.: Due sezioni stratigrafiche nel Pleistocene medio della conca di
453 Norcia; implicazioni geomorfologiche e neotettoniche. Rend. Soc. Geol. Ital. 13, 17– 26, 1990.

454 Blumetti, A. M., Dramis, F., & Michetti, A. M.: Fault-generated mountain fronts in the central Apennines (Central Italy):
455 Geomorphological features and seismotectonic implications. Earth Surface Processes and Landforms, 18(3), 203–223. doi:
456 10.1002/esp.3290180304, 1993.

457 Bohm, G., Luzi, L., Galadini, F.: Tomographic depth seismic velocity model below the plain of Norcia (Italy) for site effect
458 studies. Bollettino di geofisica Teorica ed Applicata, 2011.

459 Boncio, P., Brozzetti, F., Ponziani, F., Barchi, M., Lavecchia, G., & Pialli, G.: Seismicity and extensional tectonics in the
460 northern Umbriamarche Apennines. Memorie della Societa Geologica Italiana, 52, 539–555, 1998.

461 Boncio, P., F. Brozzetti, and G. Lavecchia: Architecture and seismotectonics of a regional low-angle normal fault zone in
462 central Italy, Tectonics, 19(6), 1038–1055, doi:10.1029/2000TC900023, 2000.

463 Bonini, L., Toscani, G., & Seno, S.: Three-dimensional segmentation and different rupture behavior during the 2012 Emilia
464 seismic sequence (Northern Italy). Tectonophysics, 630, 33-42, 2014.

465 Bonini, L., Basili, R., Burrato, P., Cannelli, V., Fracassi, U., Maesano, F. E., et al.: Testing different tectonic models for the
466 source of the Mw 6.5, 30 October 2016, Norcia earthquake (central Italy): A youthful normal fault, or negative inversion of
467 an old thrust? Tectonics, 38, doi:10.1029/2018TC005185, 2019.

468 Borre, K., Cacon, S., Cello, G., Kontny, B., Likke Andersen, H., Moratti, G., Piccardi, L., Stemberk, J., Tondi, E., Vilimek,
469 V.: The COST project in Italy: analysis and monitoring of seismogenic faults in the Gargano and Norcia areas
470 (centralsouthern Apennines, Italy). J. Geodyn. 36, 3 –18, 2003.

471 Botter, C., Cardozo, N., Hardy, S., Leconte, I., Escalona: From mechanical modeling to seismic imaging of faults: a
472 synthetic workflow to study the impact of faults on seismic. Mar. Pet. Geol. 57, 187-207, 2014.

473 Brewer, J. A., Matthews, D. H., Warner, M. R., Hall, J., Smythe, D. K., & Whittington, R. J.: BIRPS deep seismic reflection
474 studies of the British Caledonides. Nature, 305(5931), 206, 1983.

475 Brozzetti, F., & Lavecchia, G.: Seismicity and related extensional stress field: the case of the Norcia seismic zone. Annales
476 Tectonicae, 8, 38–57, 1994.

477 Brozzetti, F., Boncio, P., Cirillo, D., Ferrarini, F., de Nardis, R., Testa, A., Liberi, F., & Lavecchia, G.: High resolution field
478 mapping and analysis of the August – October 2016 coseismic surface faulting (Central Italy Earthquakes): slip distribution,
479 parameterization and comparison with global earthquakes. Tectonics, 38. https://doi.org/10.1029/2018TC005305, 2019.

Bulhões, E.M.: Técnica "Volume de Amplitudes". SBGF/6° Congresso Internacional da Sociedade Brasileira de Geofísica, Rio de Janeiro, Anais (In Portuguese), 1999.

Calamita, F., Coltorti, M., Deiana, G., Dramis, F. and Pambianchi, G.: Neotectonic evolution and geomorphology of the Cascia and Norcia depressions (Umbria-Marche Apennines), Geografia Fisica e Dinamica Quaternaria, 5, 263-276, 1982.

Calamita, F., & Pizzi, A.: Recent and active extensional tectonics in the southern Umbro-Marchean Apennines (Central Italy). Memorie della Società Geologica Italiana, 48, 541–548, 1994.

Calamita, F., Pace, P., & Satolli, S., Coexistence of fault-propagation and fault-bend folding in curve-shaped foreland fold-and-thrust belts: examples from the Northern Apennines (Italy). Terra Nova, 24(5), 396-406, 2012.

Carvalho, J., Taha, R., Cabral, J., Carrilho, F. and Miranda, M.: Geophysical characterization of the OtaVila Franca de Xira-Lisbon-Sesimbra fault zone, Portugal. Geophysical Journal International, 174, 567-584, 2008.

Cavinato, G. P., & De Celles, P. G.: Extensional basins in the tectonically bimodal central Apennines fold-thrust belt, Italy: Response to corner flow above a subducting slab in retrograde motion. Geology, 27(10), 955–958, 1999.

Centamore, E., Adamoli, L., Berti, D., Bigi, G., Bigi, S., Casnedi, R., et al.: Carta geologica dei bacini della Laga e del Cellino e dei rilievi carbonatici circostanti. In: Studi Geologici Camerti, Vol. Spec. Università degli Studi, Dipartimento di Scienze della Terra. SELCA, Firenze, 1992.

Cheloni, D., Falcucci, E., & Gori, S.: Half-graben rupture geometry of the 30 October 2016 MW 6.6 Mt. Vettore-Mt. Bove earthquake, central Italy. Journal of Geophysical Research: Solid Earth, 124. https://doi.org/10.1029/2018JB015851, 2018.

Chen, Q. and Sidney, S.: Seismic Attribute Technology for Reservoir Forecasting and Monitoring. The Leading Edge, 16 (5): 445. http://dx.doi.org/10.1190/1.1437657, 1997.

Chiarabba, C., De Gori, P., Cattaneo, M., Spallarossa, D., & Segou, M.: Faults geometry and the role of fluids in the 2016–2017 Central Italy seismic sequence. Geophysical Research Letters, 45, 6963–6971, 2018.

Chiaraluce, L., Barchi, M., Collettini, C., Mirabella, F. & Pucci, S. Connecting seismically active normal faults with Quaternary geological structures in a complex extensional environment: the Colfiorito 1997 case history (northern Apennines, Italy). Tectonics 24, TC1002, https://doi.org/10.1029/2004TC001627, 2005.

Chiaraluce, L., Di Stefano, R., Tinti, E., Scognamiglio, L., Michele, M., Casarotti, E., et al.: The 2016 Central Italy seismic sequence: A first look at the mainshocks, aftershocks, and source models. Seismological Research Letters, 88(3), 757–771. https://doi.org/10.1785/0220160221, 2017.

Chopra, S. & J. Marfurt, K.: Seismic attributes - A Historical Perspective. Geophysics. 70(5):3. https://doi.org/10.1190/1.2098670, 2005.

Chopra, S. and Marfurt, K. J.: Seismic Attributes for Prospect Identification and Reservoir Characterization. SEG Geophysical Developments Series No. 11, Stephen J. Hill, series editor and volume editor. ISBN 978-1-56080-141-2 (volume) - ISBN 978-0-931830-41-9 (series), 464 pp, 2007.

Chopra, S. & J. Marfurt, K.: Emerging and future trends in seismic attributes. The Leading Edge. 27. 298-318. 10.1190/1.2896620, 2008.

Chopra, S. and Marfurt, K.J.: Volume co-rendering of seismic attributes — A great aid to seismic interpretation, SEG Technical Program Expanded Abstracts. January 2011, 1150-1154, 2011.

Ciaccio, M., Barchi M. R., Chiarabba, C., Mirabella, F. and Stucchi E.: Seismological, geological and geophysical constraints for the Gualdo Tadino fault, Umbria-Marche Apennines (central Italy), Tectonophysics, 406, 233 – 247, 2005.

Cinti, F. R., De Martini, P. M., Pantosti, D., Baize, S., Smedile, A., Villani, F., et al.: 22-kyr-long record of surface faulting along the source of the 30 October 2016 earthquake (central Apennines, Italy), from integrated paleoseismic data sets. Journal of Geophysical Research: Solid Earth, 124, 9021– 9048. https://doi.org/10.1029/2019JB017757, 2019.

Civico, R., Pucci, S., Villani, F., Pizzimenti, L., De Martini, P. M., Nappi, R. & the Open EMERGEO Working Group: Surface ruptures following the 30 October 2016 Mw 6.5 Norcia earthquake, central Italy, Journal of Maps, 14:2, 151-160, doi: 10.1080/17445647.2018.1441756, 2018.

Coltorti, M., Farabollini, P.: Quaternary evolution of the "Castelluccio di Norcia" basin (Umbro-Marchean Apennines, central Italy). Il Quaternario 8(1), 149–166, 1995.

Cook, F. A., Albaugh, D. S., Brown, L. D., Kaufman, S., Oliver, J. E., & Hatcher Jr, R. D.: Thin-skinned tectonics in the crystalline southern Appalachians; COCORP seismic-reflection profiling of the Blue Ridge and Piedmont. Geology, 7(12), 563-567, 1979.

De Guidi, G., Vecchio, A., Brighenti, F., Caputo, R., Carnemolla, F., Di Pietro, A., et al.: Co-seismic displacement on October 26 and 30, 2016 (Mw 5.9 and 6.5) earthquakes in central Italy from the analysis of discrete GNSS network. Natural Hazards and Earth System Sciences Discussions, 2017(May), 1–11. doi: 10.5194/nhess-2017-130, 2017.

Deschamps, A., Innaccone, G., & Scarpa, R.: The Umbrian earthquake (Italy) of 19 September 1979. Annales Geophysicae, 2, 29–36, 1984.

Di, H., and AlRegib, G.: Semi-automatic fault/fracture interpretation based on seismic geometry analysis: Geophysical Prospecting, doi: 10.1111/1365-2478.12769, 2019.

DISS Working Group: Database of Individual Seismogenic Sources (DISS), Version 3.2.1: A compilation of potential sources for earthquakes larger than M 5.5 in Italy and surrounding areas. http://diss.rm.ingv.it/diss/, Istituto Nazionale di Geofisica e Vulcanologia, doi: 10.6092/INGV.IT-DISS3.2.1, 2018.

Ehsan, S. A., Carbonell, R., Ayarza, P., Martí, D., Pérez-Estaún, A., Martínez-Poyatos, D. J., Simancas, J. F., Azor, A., Mansilla, L.: Crustal deformation styles along the reprocessed deep seismic reflection transect of the Central Iberian Zone (Iberian Peninsula), Tectonophysics, 621, 159-174, https://doi.org/10.1016/j.tecto.2014.02.014., 2014.

Ehsan, S. A., Carbonell, R., Ayarza, P., Martí, D., Martínez Poyatos, D., Simancas, J. F., Azor, A., Ayala, C., Torné, M. and Pérez-Estaún, A.: Lithospheric velocity model across the Southern Central Iberian Zone (Variscan Iberian Massif): The ALCUDIA wide-angle seismic reflection transect, Tectonics, 34(3), 535-554, doi: 10.1002/2014TC003661, 2015.

Ercoli, M., Pauselli, C., Frigeri, A., Forte, E., & Federico, C.: "Geophysical paleoseismology" through high resolution GPR data: A case of shallow faulting imaging in Central Italy. Journal of Applied Geophysics, 90, 27–40. doi.org/10.1016/j.jappgeo.2012.12.001, 2013.

548 Ercoli M., Pauselli C., Frigeri A., Forte E. and Federico C.: 3-D GPR data analysis for high-resolution imaging of shallow
549 subsurface faults: the Mt Vettore case study (Central Apennines, Italy). Geophysical Journal International, 198:1(609-621).
550 doi: 10.1093/gji/ggu156, 2014.

551 Ercoli, M., Pauselli, C., Cinti, F.R., Forte, E. and Volpe, R.: Imaging of an active fault: Comparison between 3D GPR data
552 and outcrops at the Castrovillari fault, Calabria, Italy. Interpretation, 3(3), pp. SY57-SY66, 2015.

553 Ferrario, M. F., & Livio, F.: Characterizing the distributed faulting during the 30 October 2016, Central Italy earthquake: A
554 reference for fault displacement hazard assessment. Tectonics, 37, 1256–1273. https://doi.org/10.1029/2017TC004935,
555 2018.

556 Finetti, I. R., Boccaletti, M., Bonini, M., Del Ben, A., Geletti, R., Pipan, M., & Sani, F.: Crustal section based on CROP
557 seismic data across the North Tyrrhenian–Northern Apennines–Adriatic Sea. Tectonophysics, 343(3-4), 135-163, 2001.

558 Forte E., Pipan M., Casabianca D., Di Cuia R., Riva A.: Imaging and characterization of a carbonate hydrocarbon reservoir
559 analogue using GPR attributes. Journal of Applied Geophysics, 81, 76–87, 2012.

560 Forte E., Dossi M., Pipan M. and Del Ben A.: Automated phase attribute-based picking applied to reflection seismics,
561 Geophysics, 81, 2, V55-V64, doi: 10.1190/GEO2015-0333.1, 2016.

562 Galadini, F., & Galli, P.: Paleoseismology of silent faults in the central Apennines (Italy): The Mt. Vettore and Laga Mts.
563 Faults. Annals of Geophysics, 46. https://doi.org/10.4401/ag-3457, 2003.

564 Galadini, F., Falcucci, E., Gori, S., Zimmaro, P., Cheloni, D. and Stewart J. P.: Active Faulting in Source Region of 2016–
565 2017 Central Italy Event Sequence. Earthquake Spectra, 34, 4, 1557-1583, 2018.

566 Galli, P., Galadini, F., Calzoni, F.: Surface faulting in Norcia (Central Italy): a "paleoseismological perspective".
567 Tectonophysics, 403, 117–130, 2005.

568 Galli, P., Galadini, F. & Pantosti, D.: Twenty years of paleoseismology in Italy, Earth-Sci. Rev., 88(1–2), 89–117, 2008.

569 Galli,P., Galderisi, A., Ilardo, I., Piscitelli, S., Scionti, V., Bellanova, J., Calzoni, F.: Holocene paleoseismology of the
570 Norcia fault system (Central Italy), Tectonophysics, 745, 154-169, doi:10.1016/j.tecto.2018.08.008, 2018.

571 Galli, P., Galderisi, A., Peronace, E., Giaccio, B., Hajdas, I., Messina, P., et al.: The awakening of the dormant
572 Mount Vettore fault (2016 central Italy earthquake, Mw 6.6): Paleoseismic clues on its millennial silences. Tectonics, 38,
573 https://doi.org/10.1029/2018TC005326, 2019.

574 Gersztenkorn, G., Marfurt, K.J.: Eigenstructure-based coherence computations as an aid to 3-D structural and stratigraphic
575 mapping. Geophysics, 64, 1468-1479, 1999.

576 Gori, S., Falcucci, E., Galadini, F., Zimmaro, P., Stewart, J. P., Kayen, R. E., Lingwall, B., Moro, M., Saroli, M., Pizzi, A.,
577 and Di Domenica, A.: Surface faulting caused by the 2016 Central Italy seismic sequence, Earthquake Spectra 34, 1585–
578 1610, doi:10.1193/111417EQS236MR, 2018.

579 Gruppo di Lavoro Sequenza Centro Italia: Rapporto Bollettino Sismico Italiano sulla revisione dei giorni 24-26 agosto; 26-
580 27 ottobre; 30 ottobre - 1° novembre 2016. Bollettino Sismico Italiano (BSI), 13 pp., 2019.

Ha, T. N., Marfurt, K. J. and Wallet B. C., Hutchinson, B.: Pitfalls and implementation of data conditioning, attribute analysis, and self-organizing mapping to 2D data: Application to the Exmouth Plateau, North Carnarvon Basin, Australia, Interpretation, submitted, http://mcee.ou.edu/aaspi/submitted/2019/Ha_et_al_2019_Seismic_attributes_for_2D_data.pdf, 2019.

Hale, D.: Methods to compute fault images, extract fault surfaces, and estimate fault throws from 3D seismic images. Geophysics, 78(2), O33–O43, https://doi.org/10.1190/geo2012-0331.1, 2013.

Hutchinson, B.: Application and Limitations of Seismic Attributes on 2D Reconnaissance Surveys: Master's thesis, University of Oklahoma, 130 pp., 2016. https://shareok.org/handle/11244/34658.

Iacopini, D., Butler, R.W.H.: Imaging deformation in submarine thrust belts using seismic attributes. Earth Planet. Sci. Lett. 302, 414-422, 2011.

Iacopini, D., Butler, R.W.H., Purves, S.: Seismic imaging of thrust faults and structural damage: a visualization workflow for deepwater thrust belts. First Break 30, 39-46, 2012.

Iacopini, D., Butler, R. W. H., Purves, S., McArdle, N., & De Freslon, N.: Exploring the seismic expression of fault zones in 3D seismic volumes. Journal of Structural Geology, 89, 54-73, 2016.

Improta, L., Latorre, D., Margheriti, L., Nardi, A., Marchetti, A., Lombardi, A. M., Castello, B., Villani, F., Ciaccio, M. G., Mele, F. M., Moretti, M. & the Bollettino sismico Italiano Working Group: Multi-segment rupture of the 2016 Amatrice-Visso-Norcia seismic sequence (central Italy) constrained by the first high-quality catalog of early Aftershocks. Scientific Reports, 9, 6921, 2019. doi: 10.1038/s41598-019-43393-2

ISIDe working group: version 1.0; doi:10.13127/ISIDe, 2016.

Ithaca catalogue, Available at: http://www.isprambiente.gov.it/it/progetti/ suolo-e-territorio-1/ithaca-catalogo-delle-faglie-capaci, last accessed January 2019.

Koopman, A.: Detachment tectonics in the central Apennines, Italy. Geologica Eltraiectina, 30, 1–155, 1983.

Lavecchia, G.: Il sovrascorrimento dei Monti Sibillini: Analisi cinematica e strutturale. Bollettino della Società Geologica Italiana, 104, 161–194, 1985.

Lavecchia, G., Brozzetti, F., Barchi, M., Keller, J., & Menichetti, M.: Seismotectonic zoning in east-central Italy deduced from the analysis of the Neogene to present deformations and related stress fields. Geological Society of America Bulletin, 106, 1107–1120, 1994.

Lavecchia, G., Castaldo, R., de Nardis, R., De Novellis, V., Ferrarini, F., Pepe, S., Brozzetti, F., Solaro, G., Cirillo, D., Bonano, M., Boncio, P., Casu, F., De Luca, C., Lanari, R., Manunta, M., Manzo, M., Pepe, A., Zinno, I., Tizzani, P.: Ground deformation and source geometry of the 24 August 2016 Amatrice earthquake (Central Italy) investigated through analytical and numerical modeling of DInSAR measurements and structural-geological data. Geophysical Research Letters, 43, 12,389–12,398 American Geophysical Union (AGU), 2016.

Lima, R. & Teixeira, L. E. W., de Albuquerque, F. R., and Lima-Filho, F. (2018). Ground Penetrating Radar digital imaging and modeling of microbialites from the Salitre Formation, Northeast Brazil. Geologia USP - Serie Cientifica. 18. 187-200. 10.11606/issn.2316-9095.v18-146075.

Livio, F., Michetti, A. M., Vittori, E., Gregory, L., Wedmore, L., Piccardi, L., et al.: Surface faulting during the August 24, 2016, central Italy earthquake (Mw 6.0): Preliminary results. Annals of Geophysics, 59. doi: 10.4401/ag-7197, 2016.

Maesano, F. E., D'Ambrogi, C., Burrato, P., & Toscani, G.: Slip-rates of blind thrusts in slow deforming areas: examples from the Po Plain (Italy). Tectonophysics, 643, 8-25, 2015.

Mancinelli, P., Porreca, M., Pauselli, C., Minelli, G., Barchi, M. R., & Speranza, F.: Gravity and magnetic modeling of Central Italy: Insights into the depth extent of the seismogenic layer. Geochemistry, Geophysics, Geosystems, 20, https://doi.org/10.1029/2018GC008002, 2019.

Manning, T., Ablyazina, D. and Quigley, J.: The nimble node — Million-channel land recording systems have arrived. The Leading Edge, 38:9, 706-714, doi.org/10.1190/tle38090706.1, 2019.

Marfurt, K. J. Gao, D., Barnes, A., Chopra, S., Corrao, A., Hart, B., James, H., Pacht, J., Rosen, N.C.: SEPM Society for Sedimentary Geology, 31, doi: 10.5724/gcs.11.31, 2011.

Marfurt, K.J., Alves, T.M.: Pitfalls and limitations in seismic attribute interpretation of tectonic features. Interpretation 3, 5-15. http://dx.doi.org/10.1190/INT-2014-0122.1, 2015.

Marfurt, K. J.: Seismic Attributes as the Framework for Data Integration throughout the Oilfield Life Cycle, SEG, 508 pp., 2018.

Martinis, B., and Pieri, M.: Alcune notizie sulla formazione evaporitica dell'Italia centrale e meridionale. Bollettino della Società Entomologica Italiana, 4, 649–678, 1964.

Mazzotti, A., Stucchi, E., Fradelizio, G., Zanzi, L., Scandone, P.: Seismic exploration in complex terrains: A processing experience in the southern Apennines. Geophysics, 65(5), 1402–1417. https://doi.org/10.1190/1.1444830, 2000.

McArdle, N.J., Iacopini, D., KunleDare, M.A., Paton, G.S.: The use of geologic expression workflows for basin scale reconnaissance: a case study from the Exmouth Subbasin, North Carnarvon Basin, northwestern Australia. Interpretation 2, 163-177, 2014.

McClymont, A. F., Green, A. G., Villamor, P., Horstmeyer, H., Grass, C. and Nobes, D. C.: Characterization of the shallow structures of active fault zones using 3-D ground-penetrating radar data, J. Geophys. Res., 113, B10315, doi:10.1029/2007JB005402, 2008.

Milli, S., Moscatelli, M., Stanzione, O., & Falcini, F.: Sedimentology and physical stratigraphy of the Messinian turbidites deposits of the Laga basin (Central Apennines, Italy). Bollettino della Società Geologica Italiana, 126, 37–48, 2007.

Minelli, G., and Menichetti, M.: Tectonic evolution of the Perugia massifs area (Central Italy). Bollettino della Società Entomologica Italiana, 109(5), 445–453, 1990.

Mirabella, F., Barchi, M. R. and Lupattelli, A.: Seismic reflection data in the Umbria Marche region: Limits and capabilities to unravel the subsurface structure in a seismically active area. Annals of Geophysics, 51(2–3), 383–396. https://doi.org/10.4401/ag-3032, 2008.

Naeini E. Z. and Prindle, K.: Machine learning and learning from machines, The Leading Edge, 37:12, 886-893, 2018.

Patacca, E., and Scandone, P.: Late thrust propagation and sedimentary response in the thrust-belt foredeep system of the southern Apennines (Pliocene–Pleistocene). In G. Vai & I. Martini (Eds.), Anatomy of an Orogen: The Apennines and adjacent Mediterranean basins, 441–454, Norwell, MA: Kluwer Acad., 2001.

Pauselli, C., Barchi, M. R., Federico, C., Magnani, M. B. and Minelli, G.: The crustal structure of the northern Apennines (Central Italy): An insight by the CROP03 seismic line. American Journal of Science, 306(6), 428–450. https://doi.org/10.2475/06.2006.02, 2006.

Pauselli, C., Federico, C., Frigeri, A., Orosei, R., Barchi, M.R. & Basile, G.: Ground Penetrating Radar investigations to study active faults in the Norcia Basin (Central Italy), Journal of Applied Geophysics, 72, 39-45, 2010.

Pierantoni, P. P., Deiana, G., & Galdenzi, S.: Stratigraphic and structural features of the Sibillini Mountains (Umbria–Marche Apennines, Italy). Italian Journal of Geosciences, 132, 497–520. https://doi.org/10.3301/IJG.2013.08, 2013.

Pizzi, A., Calamita, F., Coltorti, M., & Pieruccini, P.: Quaternary normal faults, intramontane basins and seismicity in the Umbria-MarcheAbruzzi Apennine Ridge (Italy): Contribution of neotectonic analysis to seismic hazard assessment. Bollettino Società Geologica Italiana Special Publication, 1(January), 923–929, 2002.

Pizzi, A., Di Domenica, A., Gallovič, F., Luzi, L., & Puglia, R.: Fault segmentation as constraint to the occurrence of the main shocks of the 2016 Central Italy seismic sequence. Tectonics, 36, 2370–2387, doi:10.1002/2017TC004652, 2017.

Porreca, M., Minelli, G., Ercoli, M., Brobia, A., Mancinelli, P., Cruciani, F., Giorgetti, C., Carboni, C., Mirabella, F., Cavinato, G., Cannata, A., Pauselli, C., Barchi, M.R.: Seismic reflection profiles and subsurface geology of the area interested by the 2016–2017 earthquake sequence (Central Italy). Tectonics, 37, 1-22, doi: 10.1002/2017TC004915, 2018.

Porreca, M., Fabbrizzi, A., Azzaro, S., Pucci, S., Del Rio, L., Pierantoni, P. P., Giorgetti C., Roberts G., Barchi, M. R.: 3D geological reconstruction of the M. Vettore seismogenic fault system (Central Apennines, Italy): Cross-cutting relationship with the M. Sibillini thrust. Journal of Structural Geology, 103938, 2020.

Pucci, S, De Martini, P.M., Civico, R., Villani, F, Nappi, R., Ricci, T., Azzaro, R., Brunori, C. A., Caciagli, M., Cinti, F. R., Sapia, V., De Ritis, R., Mazzarini, F., Tarquini, S., Gaudiosi, G., Nave, R., Alessio, G., Smedile, A., Alfonsi, L., Cucci, L., Pantosti. D.: Coseismic ruptures of the 24 August 2016, Mw6.0 Amatrice earthquake (central Italy). Geophysical Research Letters, American Geophysical Union (AGU), 2017.

Ramsay, J. G., Huber, M. I.: The Techniques of Modern Structural Geology: Folds and Fractures. Elsevier Science, 391 pp., 1987.

Roure, F., P. Choukroune, X. Berastegui, J. A. Munoz, A. Villien, P. Matheron, M. Bareyt, M. Seguret, P. Camara, and J. Deramond: Ecors deep seismic data and balanced cross sections: Geometric constraints on the evolution of the Pyrenees, Tectonics, 8(1), 41–50, doi:10.1029/TC008i001p00041, 1989.

Rovida, A., Locati, M., Camassi, R., Lolli, B., & Gasperini P. (Eds.): CPTI15, the 2015 version of the parametric catalogue of Italian earthquakes, Istituto Nazionale di Geofisica e Vulcanologia. https://doi.org/10.6092/INGV.IT-CPTI15, 2016.

Schwartz, D. P., & Coppersmith, K. J.: Fault behavior and characteristic earthquakes: Examples from the Wasatch and San Andreas fault zones. Journal of Geophysical Research: Solid Earth, 89(B7), 5681-5698, 1984.

Scognamiglio, L., Tinti, E., Casarotti, E., Pucci, S., Villani, F., Cocco, M., Magnoni, F., Michelini, A., Dreger, D.: Complex fault geometry and rupture dynamics of the Mw 6.5, 2016, October 30th central Italy earthquake. J. Geophys. Res.: Solid Earth 123, 2943–2964, doi:10.1002/2018jb015603, 2018.

Serva L., Blumetti A.M., Guerrieri L. and Michetti A.M.: The Apennine intermountain basins: the result of repeated strong earthquakes over a geological time interval. Boll. Soc. Geol. It., 1, 939-946, 2002.

Simancas, J. F., Carbonell .R., González Lodeiro, F., Pérez Estaún, A., Juhlin, C., Ayarza, P., Kashubin, A., Azor, A., Martínez Poyatos, D., Almodóvar, G.R., Pascual, E., Sáez, R., Expósito, I.: Crustal structure of the transpressional Variscan orogen of SW Iberia: SW Iberia deep seismic reflection profile (IBERSEIS), *Tectonics*, 22, 1062, doi:10.1029/2002TC001479, 6, 2003.

Snieder R. and Trampert J.: Inverse Problems in Geophysics. In: Wirgin A. (eds) Wavefield Inversion. International Centre for Mechanical Sciences (Courses and Lectures), vol 398. Springer, Vienna, 1999.

Taner, M.T., Koehler, F., and Sheriff, R.E.: Complex Seismic Trace Analysis. Geophysics, 44 (6): 1041. http://dx.doi.org/10.1190/1.1440994, 1979.

Taner, M.T.: Seismic attributes. Canadian Society of Exploration Geophysicists Recorder, 26. 48-56, 2001.

Tarquini, S., Isola, I., Favalli, M., & Boschi, E.: TINITALY/01: a new triangular irregular network of Italy. Annals of Geophysics, 50–53, 2007.

Tarquini, S., Vinci, S., Favalli, M., Doumaz, F., Fornaciai, A., & Nannipieri, L.: Release of a 10-m-resolution DEM for the Italian territory: Comparison with global-coverage DEMs and anaglyph-mode exploration via the web. Computers and Geosciences, 38(1), 168–170. https://doi.org/10.1016/j.cageo.2011.04.018, 2012.

Trippetta, F., Collettini, C., Vinciguerra, S., & Meredith, P. G.: Laboratory measurements of the physical properties of Triassic evaporites from Central Italy and correlation with geophysical data. Tectonophysics, 492(1), 121–132, 2010.

Torvela T., Moreau, J., Butler, R., W. H, Korja, A. and Heikkinen, P.: The mode of deformation in the orogenic mid-crust revealed by seismic attribute analysis, Geochem., Geophys., Geosyst., 14, 1069–1086, 2013.

Vai, G. B.: Basement and early (pre-Alpine) history. In G. B. Vai & I. P. Martini (Eds.), Anatomy of an orogen: The Apennines and adjacent Mediterranean basins, 121–150, Dordrecht, Netherlands: Kluwer Academic Publisher. https://doi.org/10.1007/978-94-015-9829-3_10, 2001.

Valoroso, L. et al. Radiography of a normal fault system by 64,000 high-precision earthquake locations: The 2009 L'Aquila (central Italy) case study. J. Geophys. Res. - Solid Earth, 118, 1156–1176, https://doi.org/10.1002/jgrb.50130, 2013.

Vernengo, L., Trinchero, E., Torrejón, M. G., and Rovira, I.: Amplitude volume technique attributes and multidimensional seismic interpretation. The Leading Edge, 36(9), 776–781. https://doi.org/10.1190/tle36090776.1, 2017.

713 Villani, F., Pucci, S., Civico, R., De Martini, P. M., Cinti, F. R., & Pantosti, D.: Surface faulting of the 30 October 2016 Mw
714 6.5 central Italy earthquake: Detailed analysis of a complex coseismic rupture. Tectonics, 37, 3378–3410.
715 https://doi.org/10.1029/2018TC005175, 2018a.

716 Villani, F., Sapia, V., Baccheschi, P., Civico, R., Di Giulio, G., Vassallo, M., et al.: Geometry and structure of a fault
717 bounded extensional basin by integrating geophysical surveys and seismic anisotropy across the 30 October 2016 Mw 6.5
718 earthquake fault (central Italy): The Pian Grande di Castelluccio basin. Tectonics, 37.
719 https://doi.org/10.1029/2018TC005205, 2018b.

720 Villani, F., Maraio, S., Bruno, P.P., Improta, L., Wood, K., Civico, R., Baccheschi, P., Sapia., V., Pucci, S., Brunori, C.A.,
721 De Martini, P.M., Pantosti, D., Conti, P., Doglioni, C.: High-resolution seismic profiling of the Castelluccio basin: new
722 constraints on the shallow subsurface of the 30 October 2016 Mw 6.5 Norcia earthquake fault (central Italy). Proceeding of
723 the 38° Convegno GNGTS, 2019.

724 Wilkinson, M. W., McCaffrey, K. J. W., Jones, R. R., Roberts, G. P., Holdsworth, R. E., Gregory, L. C., et al.: Near-field
725 fault slip of the 2016 Vettore Mw 6.6 earthquake (Central Italy) measured using low-cost GNSS. Scientific Reports, 7(1),
726 4612, doi:10.1038/s41598- 017-04917-w, 2017.

727 Wrona, T., Pan, I., Gawthorpe, R. L. and Fossen, H.: Seismic facies analysis using machine learning, Geophysics, 83:5, O83-
728 O95, 2018.

729 Zhao, W., Forte, E., Fontolan, G., Pipan, M.: Advanced GPR imaging of sedimentary features: integrated attribute analysis
730 applied to sand dunes, Geophysical Journal International, 213:1, 147–156, https://doi.org/10.1093/gji/ggx541, 2018.

731

732

733   ---

Figure 1

Figure 2

737   **Figure 3**

738

Figure 4

Figure 5

743

744
745 **Figure 6**
746
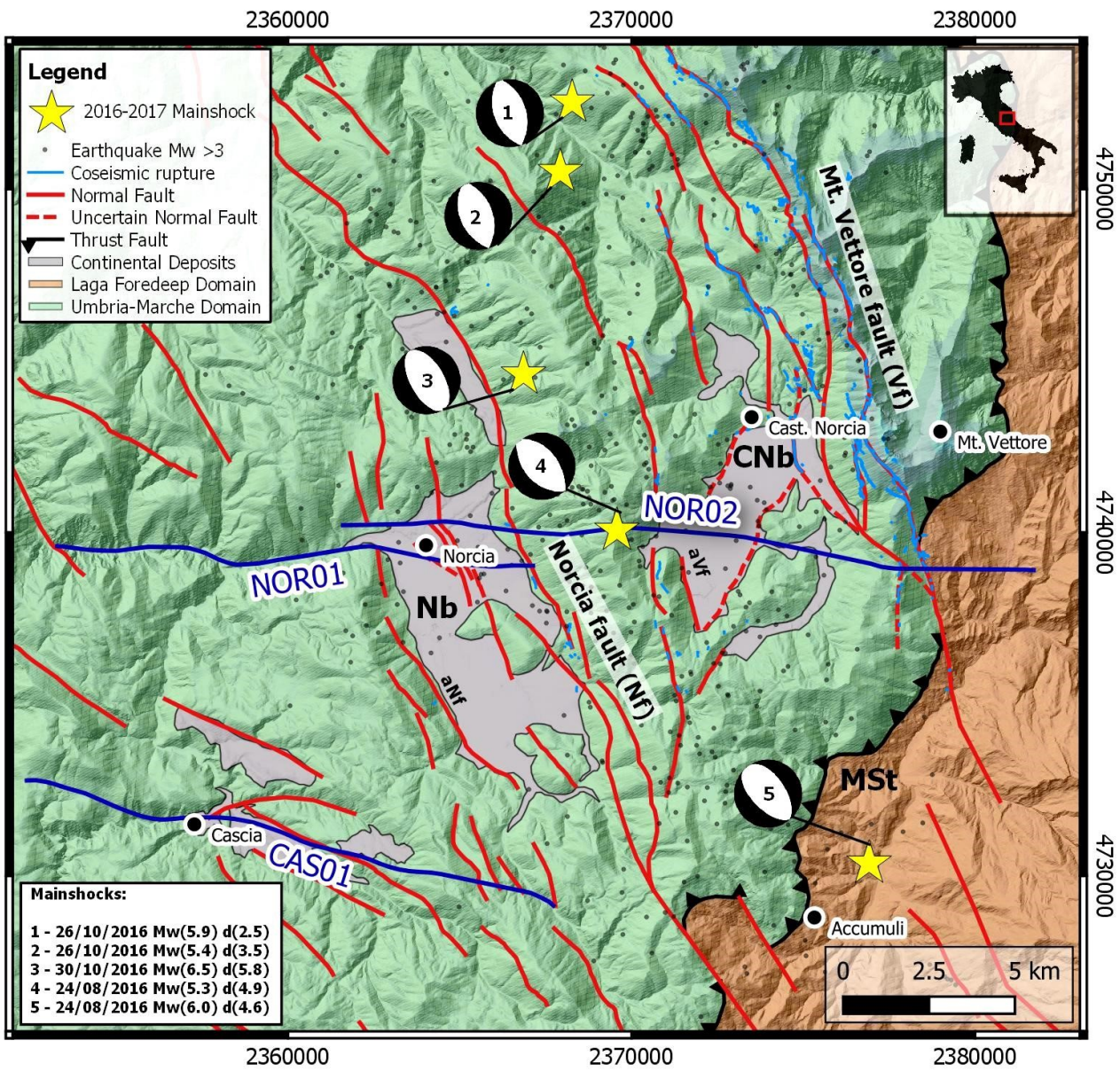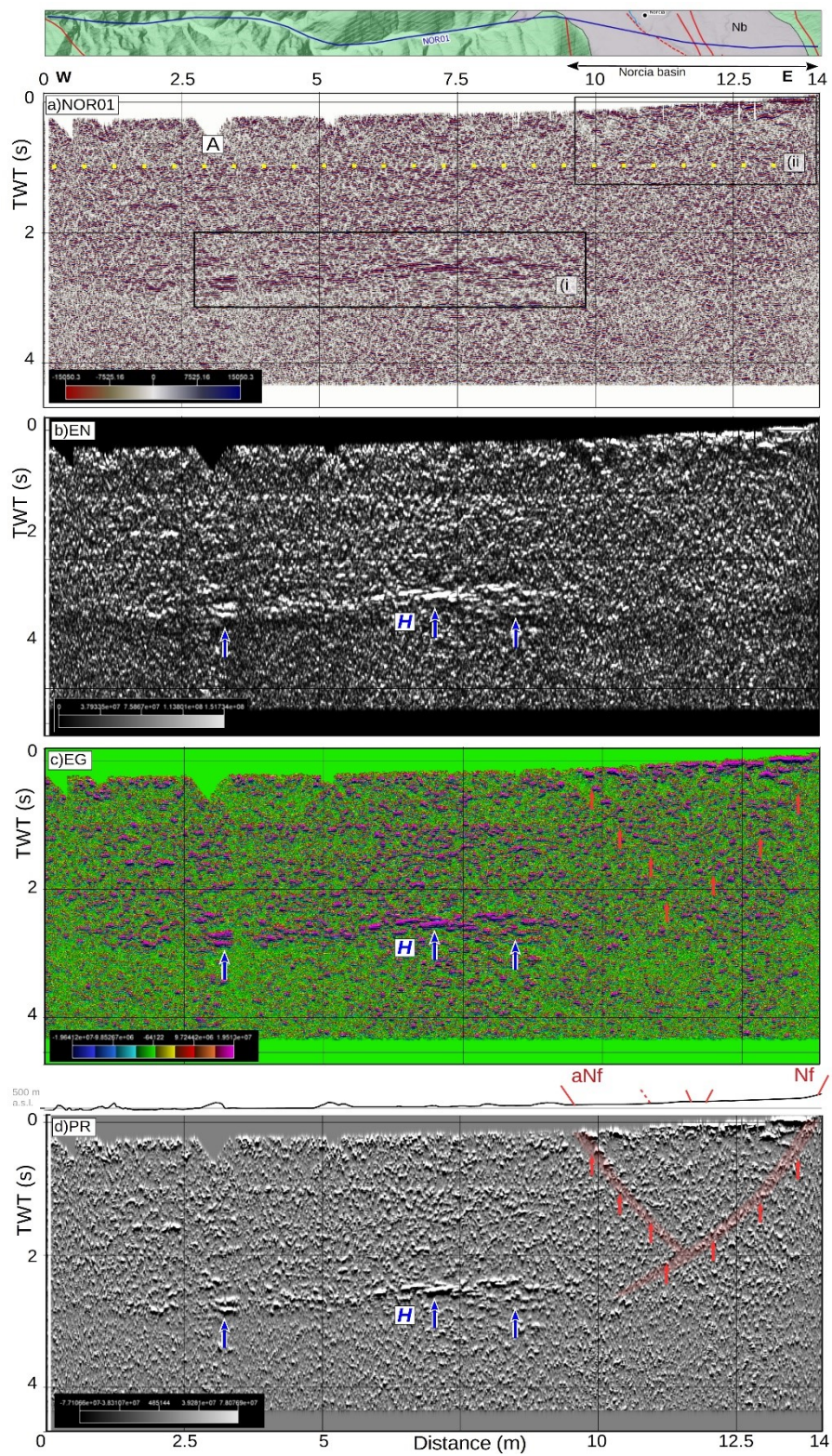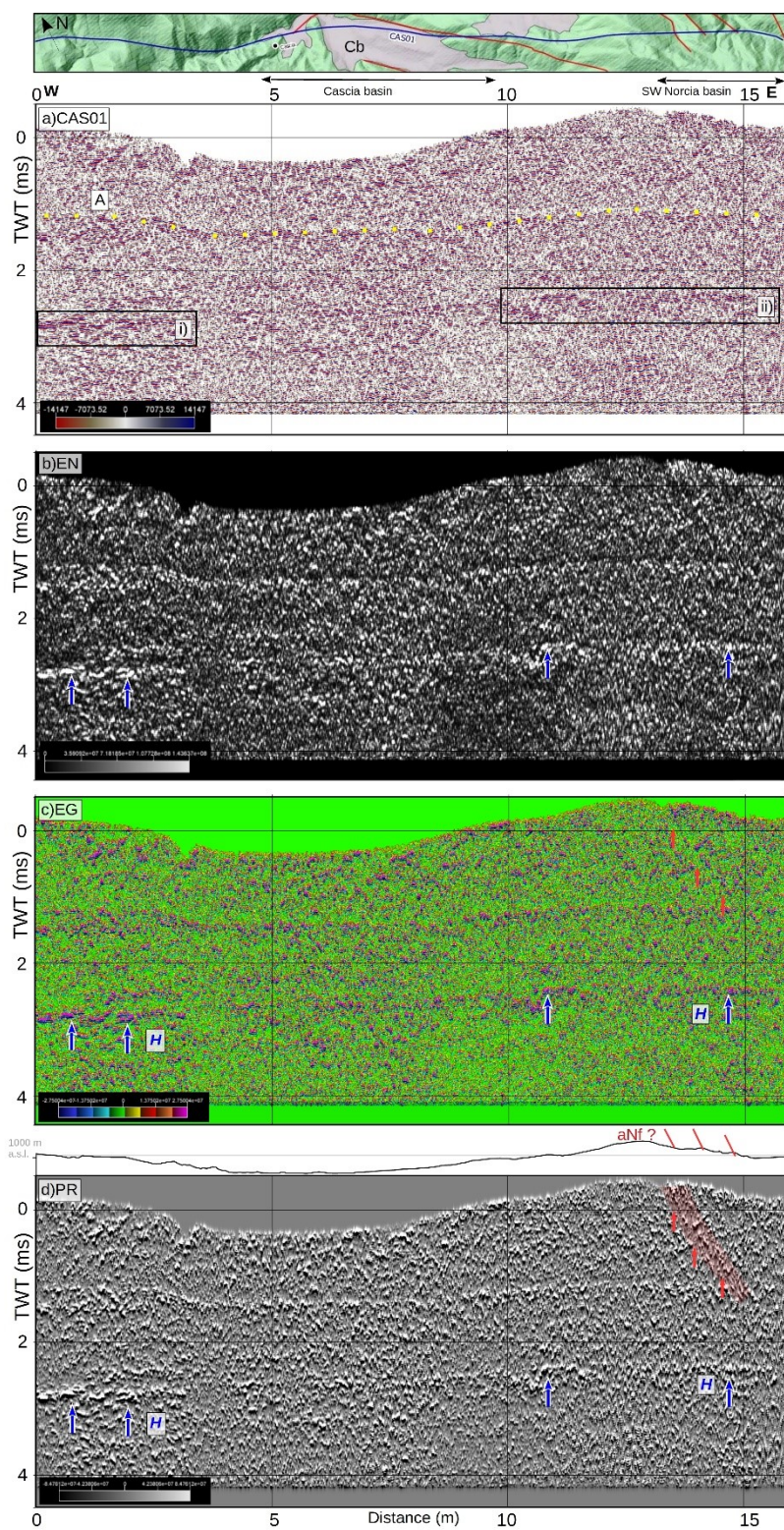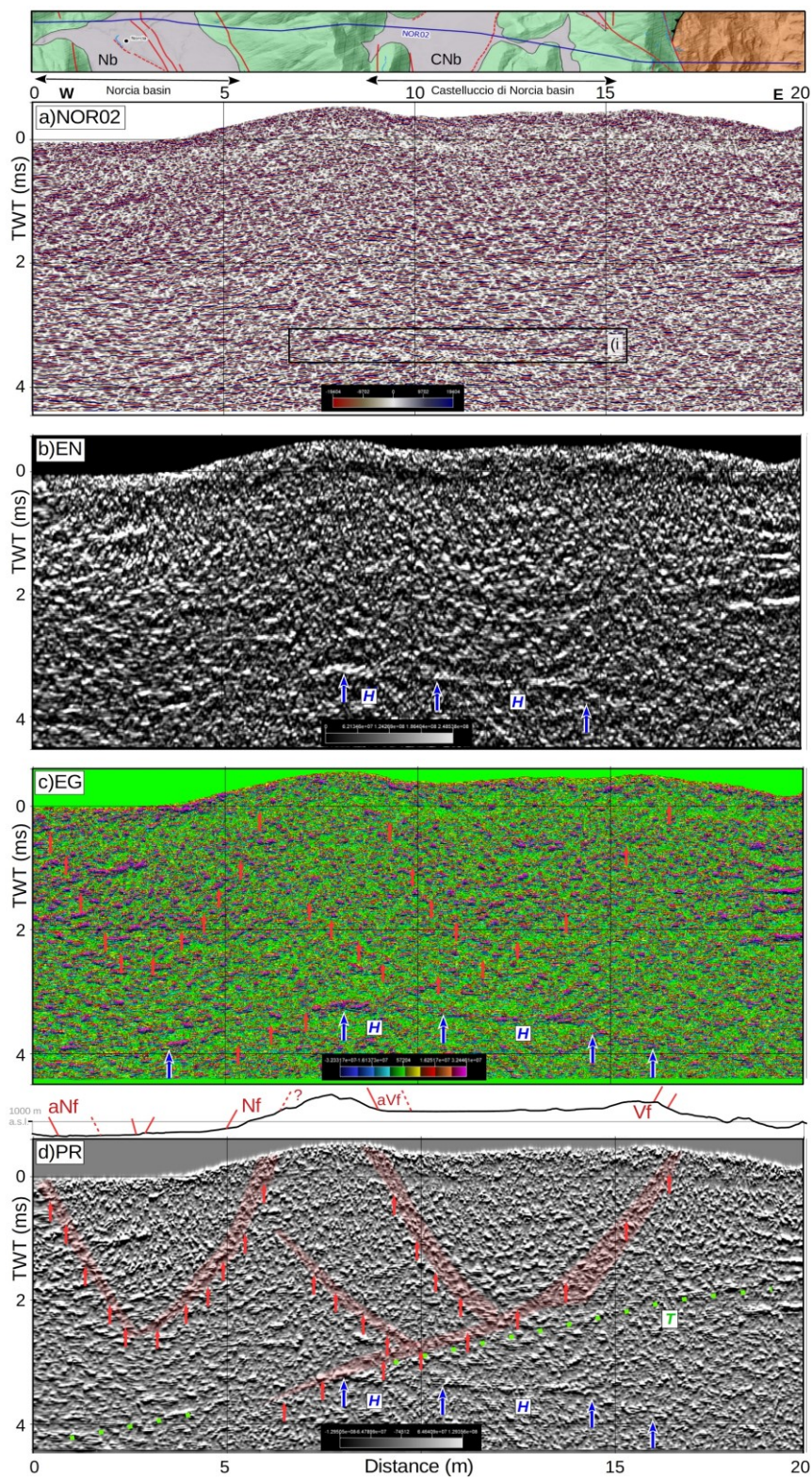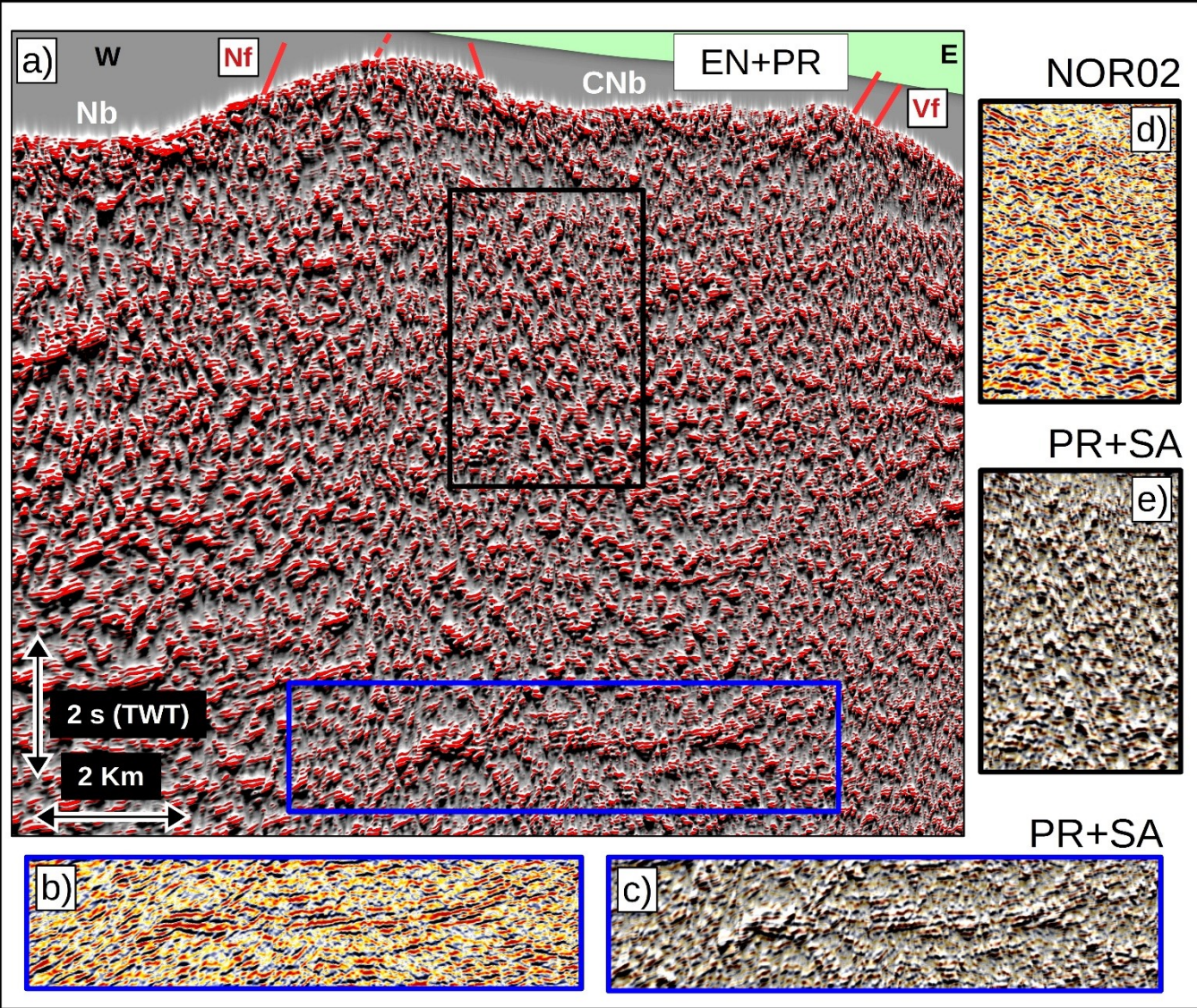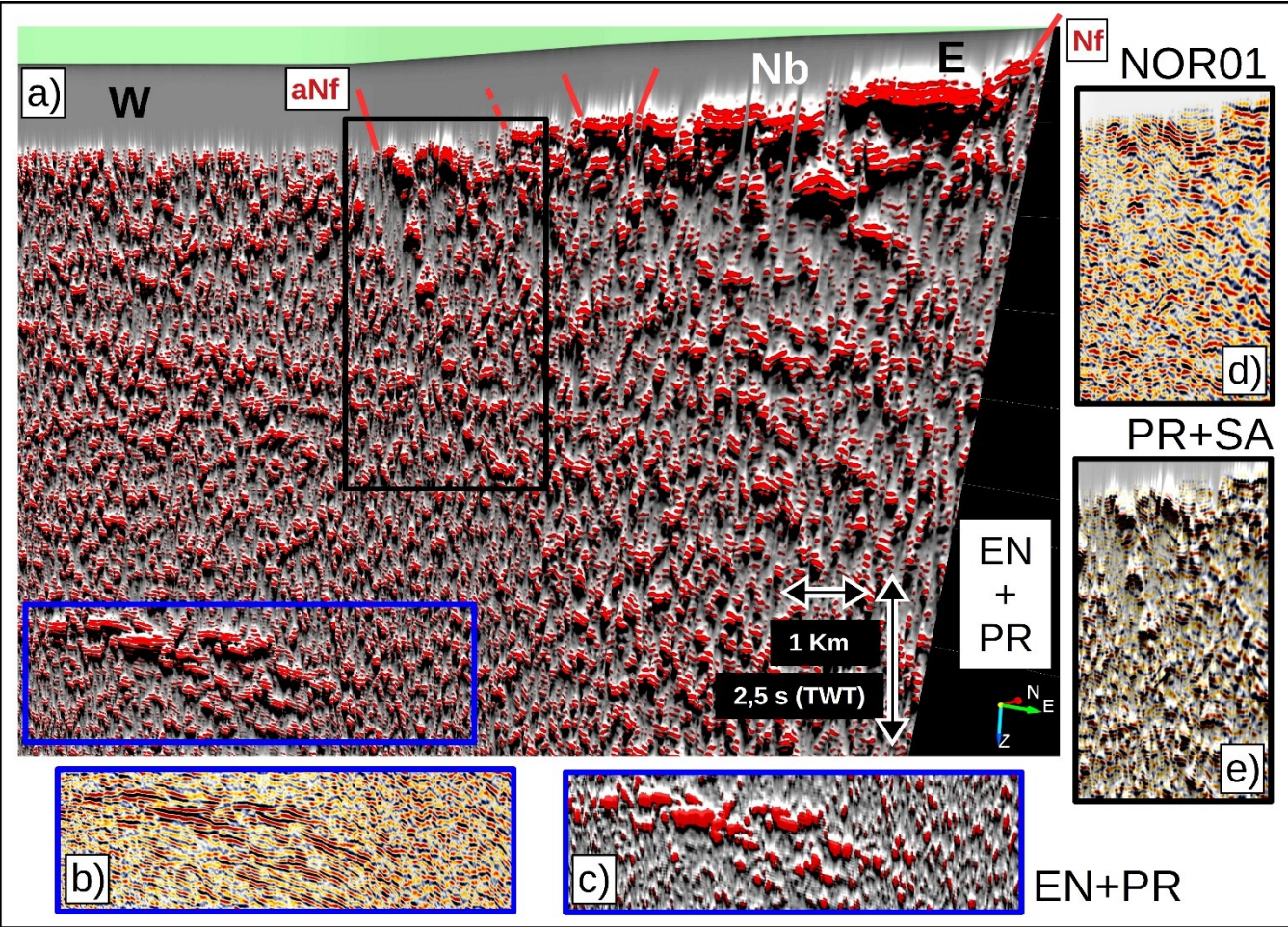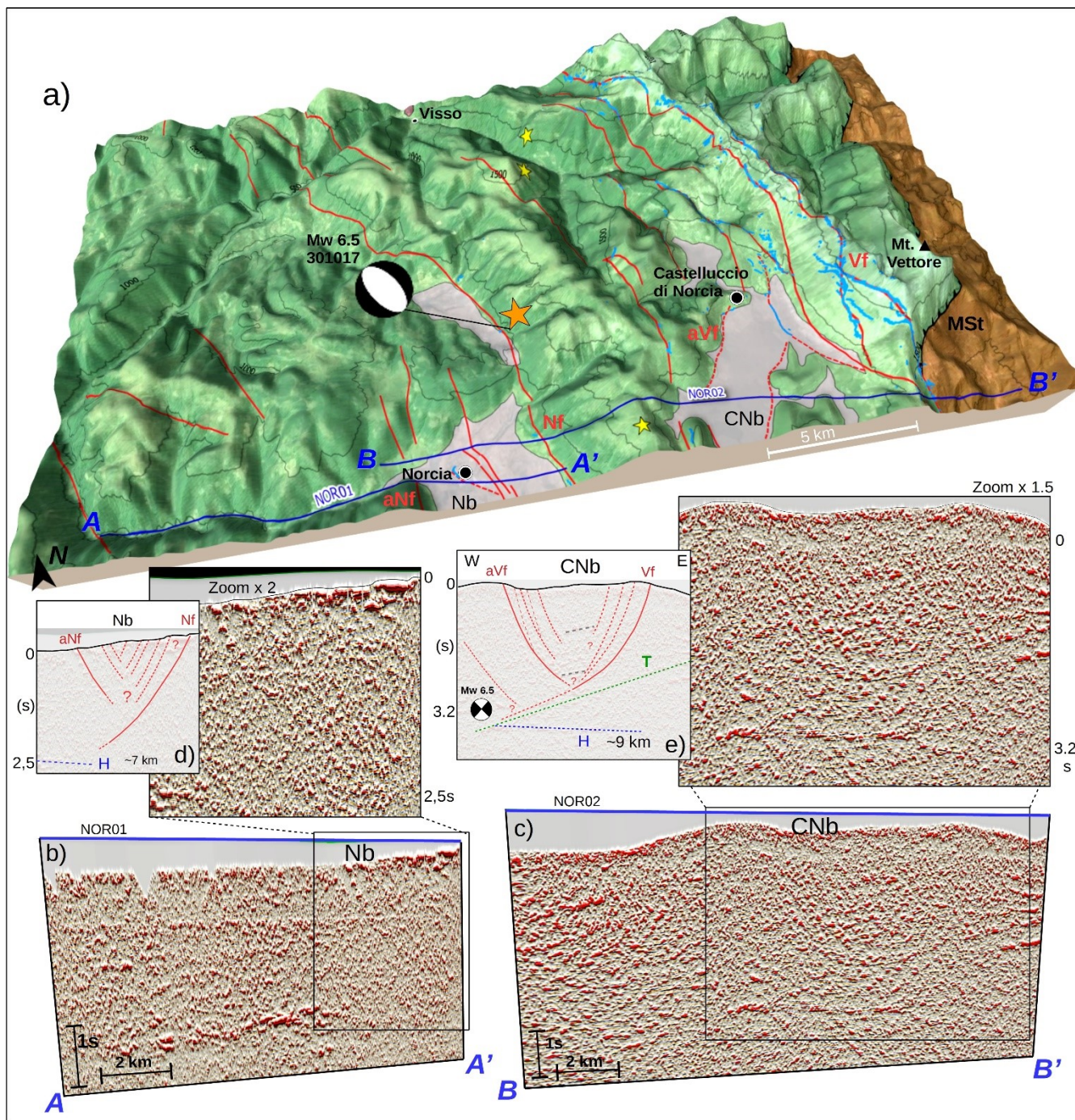
750

751
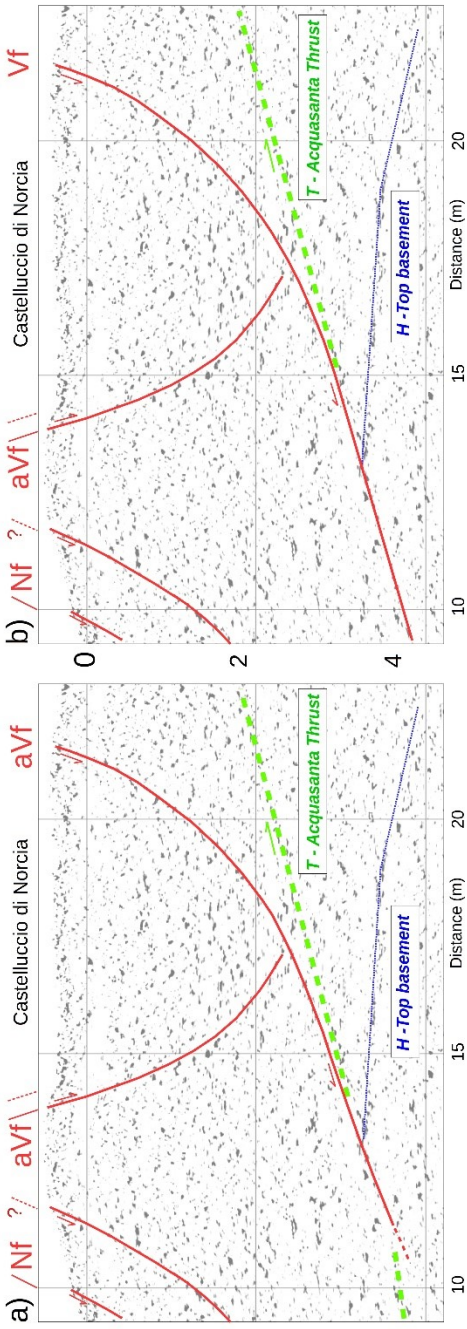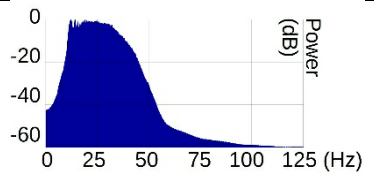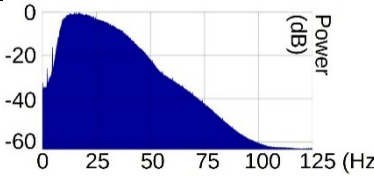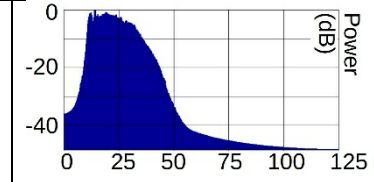
Figure 8

752

753

754   **Table 1**

Parameters	NOR01	NOR02	CAS01
Source	Vibroseis	Explosive	Vibroseis
Length (km)	14	20	16
Number of traces	938	825	1069
Samples/trace	1600	1750	1600
Time window (ms)	6400	7000	6400
Sampling interval (ms)	4	4	4
Trace interval (m)	15	25	15
Mean Spectral amplitude (dB)	Power (dB) vs Hz plot (0, -20, -40, -60; 0 25 50 75 100 125 Hz)	Power (dB) vs Hz plot (0, -20, -40, -60; 0 25 50 75 100 125 Hz)	Power (dB) vs Hz plot (0, -20, -40; 0 25 50 75 100 125 Hz)

755

756   **Figures and Tables captions:**

757   **Figure 1: Simplified geological map of the study area (modified after Porreca et al., 2018), showing the 2D seismic
758   data tracks, the 2016-2017 mainshock locations, beachballs with earthquakes magnitude, the surface ruptures and
759   the known master faults. Norcia basin (Nb), Castelluccio di Norcia basin (CNb), Monti Sibillini Thrust (MSt), Mt.
760   Vettore fault (Vf), antithetic (aVf), Norcia fault (Nf), antithetic Norcia fault (aNf).**

761   **Figure 2: Stack version of NOR01; a) standard reflection amplitude line, in the insert on the top the main faults
762   mapped at surface. The label A underlines a processing artefact whilst the boxes i) and ii) indicate the clearest
763   reflectors; b) Energy attribute enhancing a strong reflectivity contrasts (H); c) Energy Gradient, improving the
764   detection of dipping alignments and continuity of reflectors; d) Pseudo-Relief enhancing the reflection patterns cross-
765   cut by steep discontinuities. Nf Norcia fault, aNf antithetic Norcia fault at surface, yellow dots = A, blue arrows = H,
766   red arrows = indication of the main lineaments and areas with major discontinuities highlighted by the attributes.**

767   **Figure 3: Stack version of CAS01: a) standard reflection amplitude line, on the top insert the main faults mapped at
768   surface. The label A underlines a processing artefact, whilst the boxes i) and ii) indicate the main visible reflectors; b)
769   Energy attribute c) Energy Gradient attribute; d) Pseudo-Relief, showing the strong regional reflector H. A high-
770   angle discontinuity on the western margin corresponds with the southern prosecution of aNf inferred at surface. aNf
771   antithetic Norcia fault at surface, yellow dots = A, blue arrows = H, red arrows = indication of the main lineaments
772   and main signal discontinuities enhanced by the attribute's analysis.**

Figure 4: Time migrated version of NOR02; a) standard reflection amplitude line, on the top insert the main faults mapped at surface; the box i) points out the most visible reflector b) Energy attribute displaying the reflector H and a possible low angle discontinuity (T); c) Energy Gradient attribute, showing the main lineaments detected; d) Pseudo-Relief, improving the reflectors continuity/discontinuity and the display of the areas with main signal discontinuities (red polygon) after the attribute computation. Nf Norcia fault, aNf antithetic Norcia fault; Vf Mt. Vettore fault, aVf antithetic Mt. Vettore fault at surface, yellow dots = A, blue arrows = H, green dots = T, red arrows = indication of the main lineaments

Figure 5: Multi-attribute display of NOR02, displaying the position of the main faults at surface in relation to their deep seismic attribute signature; a) Energy+Pseudo-Relief attributes, the seismic facie in the blue box is compared with the original seismic line (b) and Energy+Pseudo-Relief (c) for comparison; the same plot for the black box is reported in figures d) and e) (original line and Pseudo-Relief+Standard Amplitude, respectively).

Figure 6: Multi-attribute rendering of NOR01, displaying the position of the main faults at surface in relation to their deep seismic attribute signature.; a) Energy+Pseudo-Relief attributes, the seismic facie in the blue box showing a strong set of deep reflectors is compared with the original seismic line in b) and Energy+Pseudo-Relief c). An analogous plot of the black box reports in figures d) and e) the original line and the combination Pseudo-Relief+Standard Amplitude.

Figure 7: Integration of surface and subsurface data; a) 3D-view (DTM by Tarquini et al., 2012) of a W-E section crossing the Norcia and Castelluccio di Norcia basins (Nb and CNb), and the mainshock locations (ISIDe working group, 2016). Surface and deep data allow to correlate the master faults and coseismic ruptures mapped at the surface. The multi-attribute display of NOR01 (b) and NOR02 (c), is obtained overlapping the reflection amplitude in transparency with the Pseudo-Relief and Energy attributes (red palette). The black boxes centred on Nb and CNb have been magnified for . An important improvement of the subsurface images provides additional details on the seismogenic fault zones: the sketches d) and e) show an interpretation reporting two conjugate basins, showing master faults along the borders and several minor synthetic and antithetic splays.

Figure 8: The figure proposes two alternative interpretations of the relation between the normal Vf, the deep Acquasanta thrust (T) and the Top- Basement reflector (H). Fig. 8a reports a model in which Vf merges into the deep Acquasanta thrust, suggesting a negative inversion, as a mechanism proposed by some authors (e.g. Calamita and Pizzi, 1994; Pizzi et al., 2017 Scognamiglio et al., 2018). In Fig. 8b, Vf cuts and displaces the Acquasanta thrust, following a steeper trajectory (ramp) as proposed by other authors (Lavecchia et al., 1994 and Porreca et al., 2018; 2020).

Table 1: List of some parameters extracted from SEG-Y headers and three mean frequency spectra of the three seismic lines. An approximate vertical resolution equal to 75 m was derived (v=6 km/s).

Fig.s1: Figure summarizing the three original seismic reflection profiles in amplitude used in this work.

Fig.s2: Figure 2 reporting the computed seismic attributes without any line drawing and labels.

Fig.s3: Figure 3 reporting the computed seismic attributes without any line drawing and labels.

Fig.s4: Figure 4 reporting the computed seismic attributes without any line drawing and labels.

Fig.s5: The image is a magnification of two portions of NOR01 and NOR02, focused on the two basins of Norcia and Castelluccio di Norcia, aiming to better display the discontinuities enhanced by the Pseudo Relief; a) PR on the Nb and interpretation of the primary (continuous lines) and secondary faults (dashed lines); b) PR on the CNb and interpretation of the primary (continuous lines) and secondary (dashed lines) faults bordering the basin.

The continuous red lines are the primary normal faults bounding Nb, whilst the dashed red segments compose a pattern of possible secondary splays within the basin.